nature cell biology

Prediction and validation of the distinct dynamics of transient and sustained ERK activation

Satoru Sasagawa[1,4], Yu-ichi Ozaki[1,4], Kazuhiro Fujita[2] and Shinya Kuroda[1,2,3,5]

To elucidate the hidden dynamics of extracellular-signal-regulated kinase (ERK) signalling networks, we developed a simulation model of ERK signalling networks by constraining *in silico* dynamics based on *in vivo* dynamics in PC12 cells. We predicted and validated that transient ERK activation depends on rapid increases of epidermal growth factor and nerve growth factor (NGF) but not on their final concentrations, whereas sustained ERK activation depends on the final concentration of NGF but not on the temporal rate of increase. These ERK dynamics depend on Ras and Rap1 dynamics, the inactivation processes of which are growth-factor-dependent and -independent, respectively. Therefore, the Ras and Rap1 systems capture the temporal rate and concentration of growth factors, and encode these distinct physical properties into transient and sustained ERK activation, respectively.

Transient and sustained extracellular-signal-regulated kinase (ERK) activation regulate cell fates, such as growth and differentiation, in PC12 cells[1]. Extracellular stimuli, such as epidermal growth factor (EGF) and nerve growth factor (NGF), induce transient, and transient and sustained ERK activation, respectively[1–4]. EGF-dependent ERK activation involves tyrosine phosphorylation of the EGF receptor (EGFR), SOS-dependent Ras activation[5–8], followed by activation of Raf and mitogen-activated protein kinase (MEK, also known as ERK kinase), which leads to ERK activation[9]. In turn, ERK activation is terminated by EGFR internalization, followed by degradation[10,11], recruitment of Ras GTPase-activating protein (GAP) to the plasma membrane where Ras is located[12,13], and ERK-dependent feedback inhibition of SOS[14,15], resulting in transient ERK activation. NGF-dependent ERK activation consists of transient and sustained ERK activation. NGF induces tyrosine phosphorylation of TrkA, a subunit of NGFR[1]. Transient ERK activation by NGF depends on Ras, in a similar way to EGF-dependent ERK activation[16]. Sustained ERK activation involves slow and sustained activation of Rap1 (refs 16–19), which is mediated by sustained TrkA activation[20]. Activated Rap1 activates B-Raf, followed by activation of MEK, leading to sustained ERK activation[16,17,21,22].

Recent studies have provided practical molecular frameworks of EGF- and NGF-dependent ERK signalling networks[1,18,19]; however, the dynamics of transient and sustained ERK activation remains to be elucidated. Therefore, we used an integrated approach of *in silico* kinetic simulation[23–29] and *in vivo* dynamics measurements of cross-talk points that are cooperatively regulated by upstream or downstream networks, as the dynamics of cross-talk points critically determine that of the whole networks. In addition, we used a single cell line — PC12 cells — because *in vivo* dynamics differ between cell lines due to different expression levels of molecules. We predicted and validated that the Ras and Rap1 systems specifically capture the temporal rate and concentration of growth factors, and encode these distinct physical properties of growth factors into transient and sustained ERK activation, respectively.

RESULTS

Modelling of ERK signalling networks

Based on the literature, we first developed a block diagram of ERK signalling networks (Fig. 1, and see Supplementary Information, Fig. S1). We determined kinetic parameters based on earlier experimental observations and some assumptions, then further constrained parameters on the basis of *in vivo* dynamics in PC12 cells (see Supplementary Information, Table S1).

We measured the *in vivo* tyrosine phosphorylation of EGFR and TrkA in a dose-dependent manner, using EGF and NGF, respectively, as constant stimulation of growth factors is first transformed into different temporal patterns at the receptor level (Fig. 1, boxes). The *in vivo* tyrosine phosphorylation of EGFR and TrkA were transient and sustained, respectively (Fig. 2a, b, upper panels)[18,19,30]. We next measured the *in vivo* dynamics of the cross-talk points of the ERK signalling networks (Fig. 1, boxes). Following stimulation, SOS is recruited to the plasma membrane where SOS activates Ras[31]. It is subsequently inhibited by ERK-dependent phosphorylation[32,33], leading to the dissociation of SOS from the complex with Grb2, resulting in a decline of Ras activation[32,33]. Therefore, SOS is a cross-talk point of ERK-dependent negative-feedback inhibition[32,33]. Mobility shifts in SOS reflect its phosphorylation

[1]Undergraduate Program for Bioinformatics and Systems Biology, Graduate School of Information Science and Technology, University of Tokyo, 7-3-1 Hongo, Bunkyo-ku, Tokyo 113-0033, Japan. [2]Department of Computational Biology, Graduate School of Frontier Sciences, University of Tokyo, 5-1-5 Kashiwanoha, Kashiwa 277-8583, Japan. [3]PRESTO, Japan Science and Technology Agency, 7-3-1 Hongo, Bunkyo-ku, Tokyo 113-0033, Japan.
[4]These authors contributed equally to this work.
[5]Correspondence should be addressed to S.K. (e-mail: skuroda@is.s.u-tokyo.ac.jp)

Published online: 27 March 2005; DOI: 10.1038/ncb1233

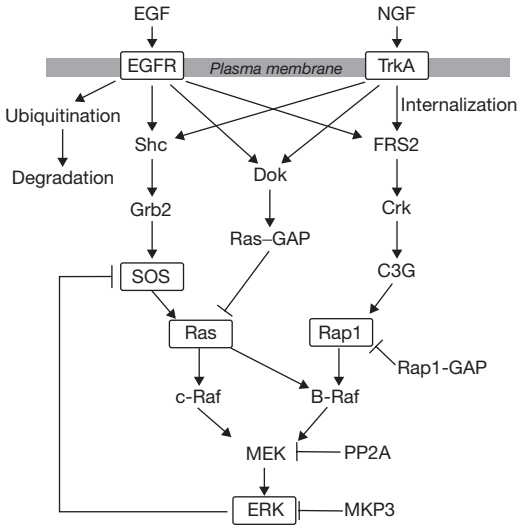

Figure 1 Schematic overview of EGF- and NGF-dependent ERK signalling networks. Arrows and bars indicate stimulatory and inhibitory interactions, respectively. *In vivo* and *in silico* dynamics of the indicated molecules were measured (boxes; see Fig. 2, and see also Supplementary Information, Fig. S2). All the biochemical reactions and parameters are provided in Supplementary Information, Fig. S1 and Table S1, respectively. MKP3, MAP kinase phosphatase 3; PP2A, protein phosphatase 2A.

state, which can be regarded as an inactive state of SOS[32,33]. The *in vivo* mobility shifts of SOS, in response to EGF and NGF, were correlated with ERK activation[18,32,33] (Fig. 2e, f, and see Supplementary Information, Fig. S2). Signals downstream of the receptors diverge into Ras and Rap1 activities, then merge again into ERK activation[16,17] via successive Raf and MEK activation[9,34]. These small GTPases are activated by the conversion of GDP-bound forms to GTP-bound forms[35]. The *in vivo* activation of Ras was transient in response to both stimuli (Fig. 2c, upper panel)[18,19]. The EGF stimulus did not induce sufficient activation of Rap1, whereas the NGF stimulus induced sustained activation of Rap1 (Fig. 2d, upper panel)[18,19]. The EGF stimulus induced transient ERK phosphorylation *in vivo* (Fig. 2e, upper panel), whereas the NGF stimulus induced transient and sustained ERK phosphorylation *in vivo* (Fig. 2f, upper panel)[18,19].

We fixed the parameters by constraining the corresponding *in silico* dynamics on the basis of the above *in vivo* dynamics (Fig. 2, lower panels, and see Supplementary Informtion, Table S1). Of note, transient ERK activation did not always correlate with tyrosine phosphorylation of EGFR, especially at low doses of EGF *in vivo* and *in silico* (Fig. 2a, e), whereas the sustained ERK activation was nearly proportional to the tyrosine phosphorylation of TrkA *in vivo* and *in silico* (Fig. 2b, f, and see below). The *in silico* EGF-dependent transient ERK phosphorylation mainly depended on Ras activation, whereas the *in silico* NGF-dependent transient and sustained ERK phosphorylation depended on Ras and Rap1 activation, respectively[16,17] (see Supplementary Information, Fig. S3h, i). We further examined the dynamics without changing parameters.

Prediction and validation of the distinct ERK dynamics

Constant stimulation of growth factors is generally used for *in vivo* dynamics measurements (Fig. 3a, b, upper panels, solid lines). However, under physiological conditions, concentrations of growth factors are likely to gradually increase in a spatiotemporal-dependent manner. Therefore, we predicted ERK activation in response to various increasing rates of EGF and NGF (Fig. 3a, b, upper panels). Although constant EGF stimulus induced transient ERK activation, transient ERK activation gradually decreased as the temporal rates of EGF decreased *in silico* (Fig. 3a, middle panel). Importantly, the slow stimulus did not induce sufficient transient ERK activation (Fig. 3a, middle panel, green dashed line). By contrast, a similar sustained ERK activation was induced by both increasing and constant NGF stimuli *in silico* (Fig. 3b, middle panel). However, transient ERK activation gradually decreased as the temporal rates of NGF decreased. Therefore, transient ERK activation depends on the temporal rates of EGF and NGF, whereas sustained ERK activation can respond to both increasing and constant NGF stimuli and depends on the final concentrations. This difference is due to the distinct activation and inactivation mechanisms of Ras and Rap1 (see below).

We next attempted to validate this *in silico* prediction by measuring *in vivo* dynamics. As predicted, transient ERK activation decreased as the temporal rate of EGF decreased *in vivo* (Fig. 3a, lower panel). The slow stimulus did not induce sufficient transient ERK activation (Fig. 3a, lower panel, green dashed line). As the temporal rate of EGF decreased, the peak concentration of transient ERK phosphorylation decreased *in silico* (Fig. 3c). By contrast, a similar sustained ERK activation was induced by both increasing and constant NGF stimuli *in vivo* (Fig. 3b, lower panel). However, transient ERK activation gradually decreased as the temporal rates of NGF decreased, which was also consistent with the *in silico* prediction. Sustained ERK activation depends on the final concentrations of NGF, irrespective of constant or increasing stimulation *in silico* (Fig. 3d).

We further performed stepwise increases and decreases of stimuli to predict *in silico* dynamics and to validate the dynamics of ERK activation *in vivo* (Fig. 4). The stepwise increase of EGF successively triggered transient ERK activation *in silico* and *in vivo* (Fig. 4a). The initial constant EGF stimulus (0.5 ng ml^{-1}) triggered efficient transient ERK activation, and the additional constant EGF stimulus (10 ng ml^{-1}) again triggered transient ERK activation, indicating that the rapid increase of EGF, rather than a threshold or absolute concentration, induces transient ERK activation. A stepwise decrease of NGF, however, induced sustained ERK activation that was similar to that seen in response to the final concentration, rather than the initial concentration, of NGF *in silico* and *in vivo* (Fig. 4b)[36].

Therefore, these results clearly indicate that transient ERK activation depends on the rapid temporal rates of growth factors but not on their final concentrations, whereas sustained ERK activation depends on the final concentration of NGF but not on its temporal rate of increase.

Distinct temporal dynamics of Ras and Rap1 activation

We explored the mechanisms underlying the distinct dynamics of transient and sustained ERK activation *in silico* (Fig. 5). Transient ERK activation, which requires a rapid increase of stimuli, is due to the mechanism of Ras activation. Transient Ras activation decreased as the temporal rate of growth factors decreased (Fig. 5a, lower panel). The slow EGF stimulus did not induce sufficient transient Ras activation (Fig. 5a, green dashed line in lower panel). Transient Ras activation is determined by the balance between activation and inactivation processes. Deletion of Ras–GAP activity resulted in sustained Ras activation (see Supplementary Information, Fig. S3), indicating that Ras–GAP is crucial for the rapid termination of transient Ras activation. Inhibition of either EGFR internalization or ERK-dependent feedback inhibition of SOS did not affect transient Ras activation (see Supplementary Information, Fig. S3). Therefore, transient Ras

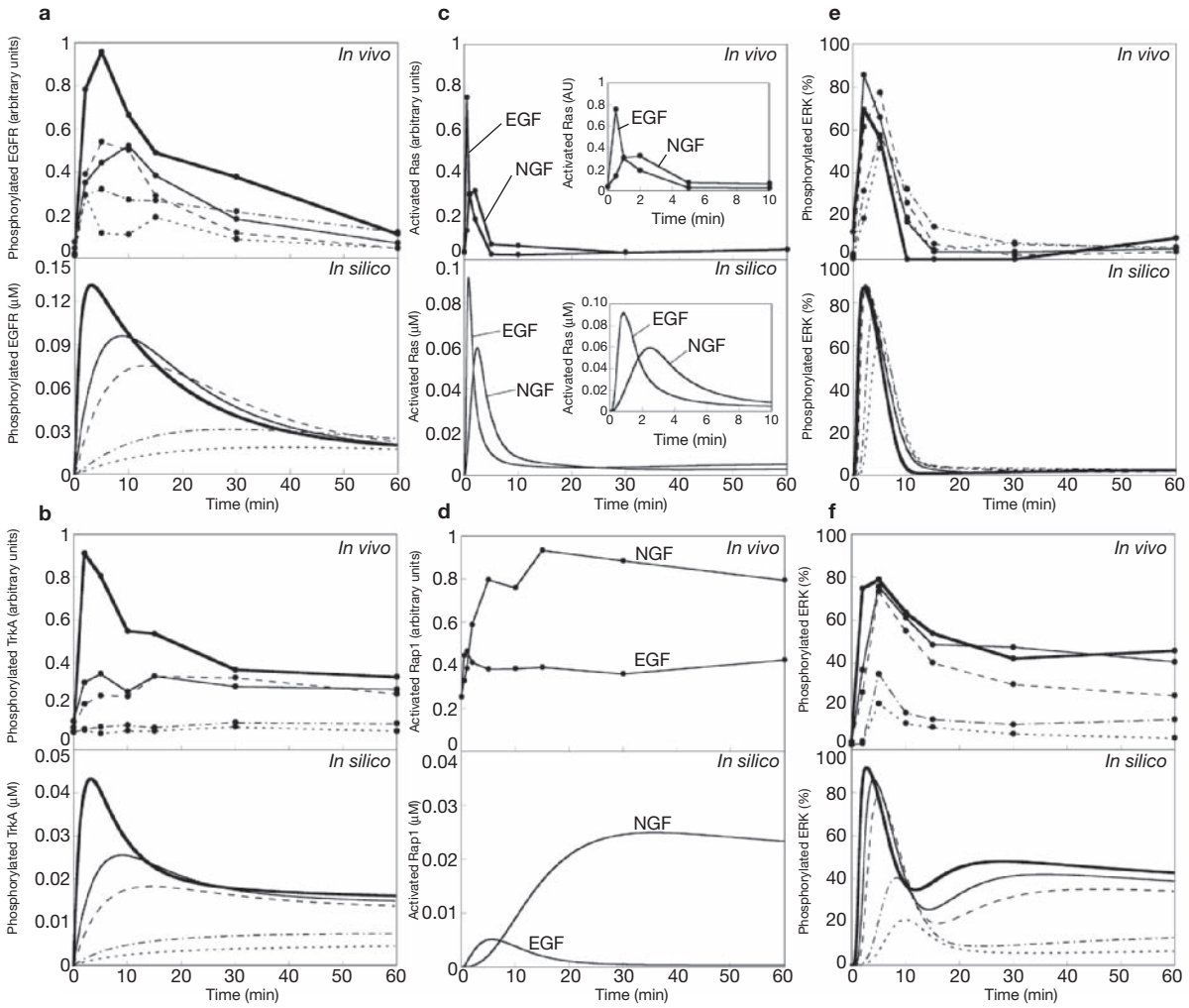

Figure 2 *In vivo* and *in silico* dynamics of ERK signalling networks. *In vivo* (upper panel) and *in silico* (lower panel) tyrosine phosphorylation of epidermal growth-factor receptor (EGFR; **a**) and TrkA (**b**), activation of Ras (**c**) and Rap1 (**d**), and EGF- (**e**) and nerve growth factor (NGF)- (**f**) dependent phosphorylation of ERK. Insets in **c** show transient Ras activation within 10 min after stimulation. The thick line, thin line, thin dashed line, thin dash-dotted line and thin dotted line indicate the responses with a constant 50, 10, 5, 1 and 0.5 ng ml^{-1} of either EGF or NGF, respectively, except for Ras and Rap1 activation. For Ras and Rap1 activation, 10 ng ml^{-1} of EGF or NGF was used. The results are representative of three independent experiments. Images of the original gels of the immunoblotting are shown in Supplementary Information, Fig. S2.

activation is substantially regulated by the activity balance between SOS[31] and Ras–GAP[12,13] in the *in silico* model. The rapid stimuli, as the constant stimuli, initially led to fast SOS recruitment (Fig. 5a, upper panel) and then to slow Ras–GAP recruitment *in silico* (Fig. 5a, middle panel), resulting in sufficient transient Ras activation *in silico* (Fig. 5a, lower panel). Although the slow stimuli led to the same processes, differences in activity between SOS and Ras–GAP were extended and decreased *in silico*, resulting in the disappearance of transient Ras activation. The apparent time constants of SOS and Ras–GAP recruitment mainly depended on the time constants of binding of Shc to phosphorylated EGFR, and of phosphorylation and dephosphorylation of Dok, respectively, *in silico* (data not shown). The amplitudes of SOS and Ras–GAP recruitments mainly depended on the affinities of Shc to SOS–Grb2, and of phosphorylated Dok to Ras–GAP, respectively, and also on the initial concentrations of Shc and Ras–GAP, respectively, *in silico* (data not shown). Consistent with this *in silico* prediction, the *in vivo* recruitment of SOS to the membrane fraction preceded that of Ras–GAP in response to the constant EGF stimulus (Fig. 5c). Therefore, transient Ras activation depends on a temporal rate of growth factors.

In contrast to Ras–GAP, Rap1–GAP was constant regardless of the stimuli *in silico*. An apparent negative-feedback inhibition and stimuli-dependent inactivation process has not been found in the Rap1 activation process, and therefore Rap1 activation simply responded to the C3G activity, which depended on sustained TrkA phosphorylation (Fig. 5b). Therefore, Rap1 can respond to both an increase and a decrease of NGF stimulus and the activation of Rap1 depends on the final concentration of NGF (Fig. 5b). Consistent with this *in silico* prediction, sustained Rap1 activation was observed in response to both constant and increasing NGF stimuli *in vivo* (Fig. 5b, lower panel). We also found that sustained Ras or Rap1 activation can lead to sustained ERK activation *in silico* (see Supplementary Information, Fig. S3), and sustained EGFR phosphorylation induced by EGF (10 ng ml^{-1}) in the presence of MG-132 (ref. 37), a proteasome inhibitor, increased sustained Ras, Rap1 and ERK activation *in vivo* (see Supplementary Information, Fig. S4).

These results indicate that the growth-factor-dependent fast SOS and slow Ras–GAP activation regulates transient Ras activation, and that the growth-factor-dependent C3G activation with the constant Rap1–GAP activity regulates sustained Rap1 activation.

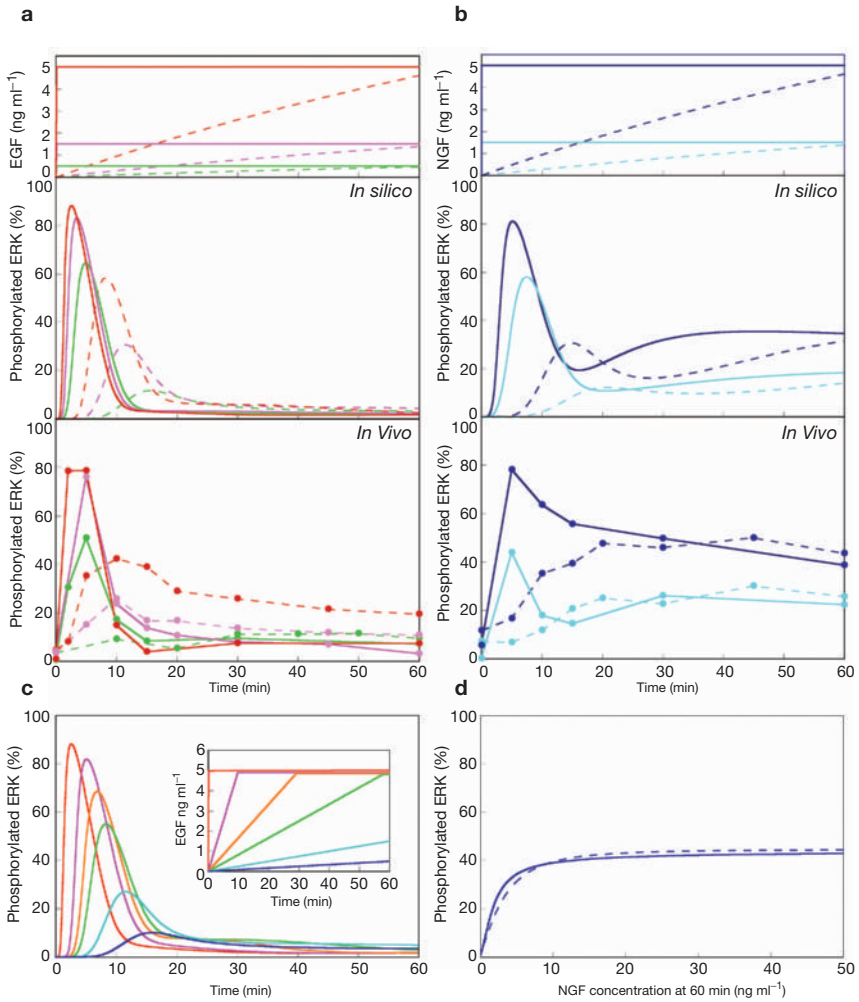

Figure 3 Distinct dynamics of transient and sustained ERK activation. For epidermal growth factor (EGF, **a**) and nerve growth factor (NGF, **b**), the indicated stimuli (upper panels) were given and the extracellular-signal-regulated kinase (ERK) phosphorylation *in silico* (middle panels) and *in vivo* (lower panels) was plotted. The constant and increasing stimuli, and the corresponding responses are indicated by solid and dashed lines, respectively. The images of the original gels in **a** and **b** are shown in Supplementary Information, Fig. S2. (**c**) The temporal rate of EGF-dependent ERK phosphorylation *in silico*. The indicated EGF stimuli (inset) were given and the transient ERK activation was plotted. (**d**) The *in silico* sustained ERK phosphorylation at 60 min. Solid and dashed lines indicate ERK phosphorylation at 60 min with constant and increasing NGF stimuli, respectively. The increasing stimuli are represented as the NGF concentrations at 60 min.

Mechanisms of the Ras and Rap1 systems

To facilitate understanding of the dynamics of the Ras and Rap1 systems, we developed simple Ras and Rap1 models downstream of phosphorylated receptors (Fig. 6; see also Methods.) In the simple Ras model, Ras activation and inactivation were approximated by reactions with pR (phosphorylated receptor)–GEF and by reaction with pR–GAP, respectively (Fig. 6a, equtions (3)–(5). We simplified the equations further by substituting variables with dimensionless variables, yielding equations (3')–(5'), where *GEF*, *GAP*, *Ras* and *Rap1* are dimensionless representations of pR–GEF, pR–GAP, Ras–GTP and Rap1–GTP, respectively. We found that the simple Ras model, with equivalent parameters in the *in silico* model, was similar to the *in silico* dynamics of Ras activation (Fig. 6b red line, see also Fig. 7a). Here, q is the relative rate constant of *GAP* activation compared with *GEF* activation (see Supplementary Information, Fig. S5), and therefore $q<1$ and $q>1$ indicate the conditions in which *GEF* activation is faster and slower than *GAP* activation, respectively. The apparent transient peak of *Ras* was observed with $q<1$, but not with $q>1$, in response to constant *pR* stimulation (Fig. 6b). Furthermore, transient *Ras* activation, defined by $Ras_{transient}$ (see Supplementary Information, Fig. S5), was induced in a temporal rate (r)-dependent manner in *pR* increase (Fig. 6c). By contrast, in the simple Rap1 model (see below), transient *Rap1* activation was not observed under any condition (data not shown). This result supports the idea that the fast SOS and subsequent slow Ras–GAP activation enables the Ras system to capture the temporal rate of stimulation.

We also developed a simple Rap1 model, in which Rap1 activation and inactivation were approximated by reaction with pR–GEF and by reaction with constant GAP, respectively (Fig. 6d). We derived equation (1) for *Rap1* activation at steady state from equations (3') and (4') (Fig. 6e):

$$Rap1 = \frac{pR}{(1+Ke)\,pR + Ke} \qquad (1)$$

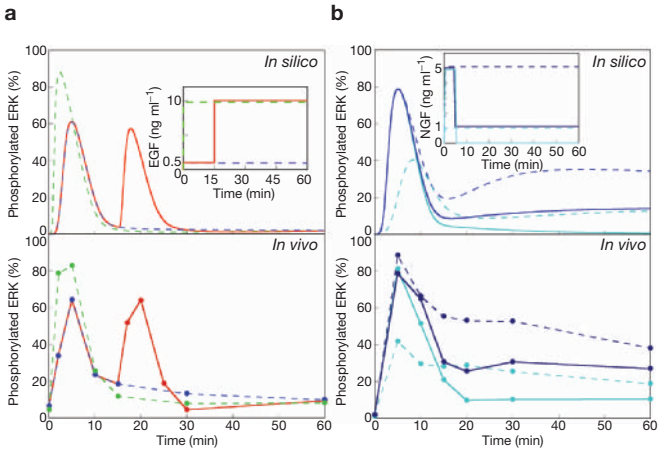

Figure 4 *In silico* and *in vivo* ERK activation in response to stepwise increases of EGF and to stepwise decreases of NGF. (**a**) The indicated stepwise increase of epidermal growth factor (EGF) stimulus (**inset**) was performed and extracellular-signal-regulated kinase (ERK) phosphorylation *in silico* (upper panel) and *in vivo* (lower panel) was plotted. The solid red line indicates the stepwise increases in EGF stimulus (0.5–10 ng ml^{-1}). The dashed blue and green lines indicate 0.5 and 10 ng ml^{-1} of constant EGF stimuli, respectively. (**b**) The indicated stepwise decrease of nerve growth factor (NGF) or constant NGF stimulus (inset) was performed and ERK phosphorylation *in silico* (upper panel) and *in vivo* (lower panel) was plotted. The solid blue and cyan lines indicate the stepwise decreases of NGF stimuli (5–1 ng ml^{-1} and 5–0 ng ml^{-1}, respectively). The dashed blue and cyan lines indicate 5 and 1 ng ml^{-1} of constant NGF stimuli, respectively. The images of the original gels in **a** and **b** are shown in Supplementary Information, Fig. S2.

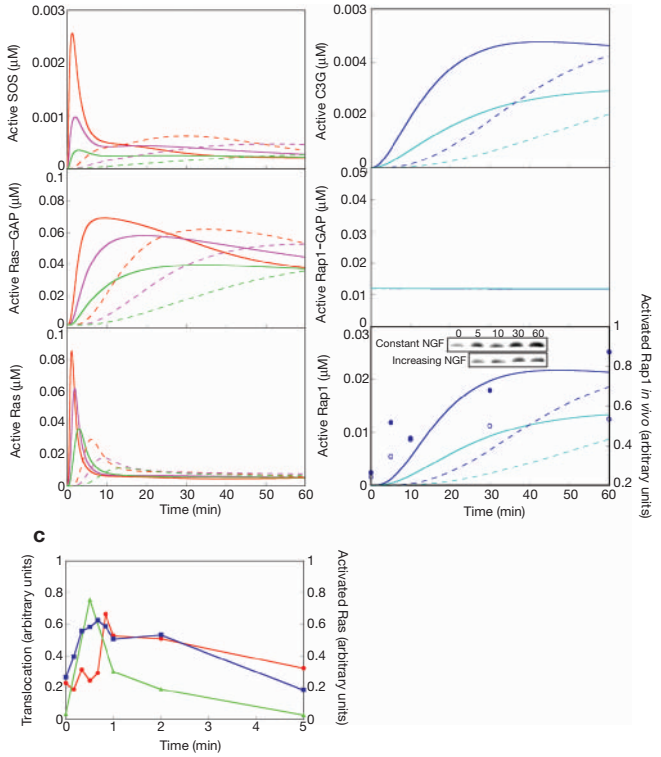

Figure 5 Distinct dynamics of EGF- and NGF-dependent Ras and Rap1 activation. The same stimuli as those shown in Fig. 3 were given, and (**a**) the epidermal growth factor (EGF)-dependent active fractions of SOS (upper panel), Ras–GAP (middle panel) and Ras (lower panel), and (**b**) the nerve growth factor (NGF)-dependent active fractions of C3G (upper panel), Rap1–GAP (middle panel) and Rap1 (lower panel) were plotted *in silico*, except that closed and open circles in **b** (lower panel) indicate the activated Rap1 *in vivo* in response to constant and increasing NGF stimuli (5 ng ml^{-1} at 60 min), respectively. Lines and colours are the same as in Fig. 3. Images of the original gels of the immunoblotting are shown in the inset. (**c**) *In vivo* recruitment of SOS and Ras–GAP to the membrane fraction in response to constant EGF stimulus. A constant EGF stimulus (10 ng ml^{-1}) was given, and the amounts of SOS (blue) and Ras–GAP (red) in the membrane fractions were measured. The *in vivo* activated Ras in Fig. 2c were also plotted (green). The images of the original gels in **c** are shown in Supplementary Information, Fig. S2.

where pR is given by a constant, α (see Methods). Under the conditions, such as $\alpha << 1$, in which the *GEF* activation was not saturated (Fig. 5b; also see Supplementary Information, Fig. S5), equation (1) can be approximated by:

$$Rap1 = \frac{pR}{Ke} \qquad (1')$$

This approximation clearly highlights the characteristics of *Rap1* activation at steady state, which is proportional to pR (Fig. 6e). This result supports the idea that constant Rap1–GAP activity, with stimulation-dependent C3G activation, enables the Rap1 system to capture the final concentration of stimulation.

We also derived equation (2) for *Ras* activation at steady state:

$$Ras = \frac{1}{1 + pKe\,\dfrac{1+pR}{1+p\times pR}} \qquad (2)$$

where pR is given by a constant, α, and p is the constant, which is the ratio of the dissociation constants between pR for GEF and pR for GAP (Fig. 6f). Under the conditions of $\alpha << 1$ and $p\alpha << 1$, whereby the *GEF* and *GAP* activations were not saturated (Fig. 5a; also see Supplementary Information, Fig. S5), equation (2) can be approximated by:

$$Ras = \frac{1}{1 + pKe} \qquad (2')$$

This approximation clearly highlights the characteristics of *Ras* activation at steady state, which becomes constant and independent of pR (Fig. 6f). The slope of the plot of *Ras* activation, which corresponds to the order of the reactions from pR to *Ras* activation, was lower than that of *Rap1* activation under the conditions, such as $\alpha << 1$ and $p\alpha << 1$ (Fig. 6e, f), thereby characterizing the distinct dynamics between the *Ras* and *Rap1* activation at steady state.

Next, we confirmed the above characteristics *in silico* (Fig. 7). Responses of transient Ras activation versus the indicated values of q and r *in silico* were very similar to those in the simple Ras model (Figs 6b, c; 7a, b), where q, r and $Ras_{transient}$ denote the relative rate constant of Ras–GAP activation compared with SOS activation, increasing the rate of phosphorylated EGFR and the relative peak amplitude of transient Ras activation, respectively (see Supplementary Information, Fig. S5). These results indicate that the simple Ras model retains the essential characteristics of transient Ras activation *in silico*.

We also confirmed that the simple Rap1 and Ras models represent the same characteristics of Rap1 and Ras activation at steady state *in silico*. The slopes of the plot of Rap1 activation versus both phosphorylated receptors at steady state were very similar at lower doses *in silico* (Fig. 7c). The slopes of the plots of Ras activation versus both phospho-

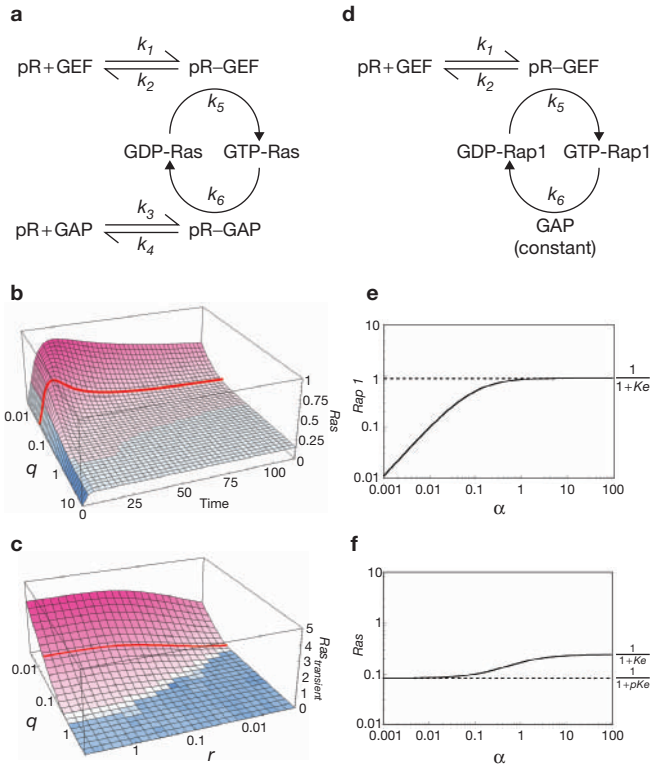

Figure 6 Characteristics of Ras and Rap1 activation in the simple Ras and Rap1 models. (**a**) Simple Ras model, in which pR-dependent GEF and GAP activation regulate Ras activation. (**b**) Constant *pR* stimulation was given, and *Ras* was plotted against the indicated values of *q*. Here, time denotes t/k_2. (**c**) $Ras_{transient}$ was plotted against the indicated values of *r* and *q*, where $Ras_{transient}$ and *r* indicate the relative peak amplitude of transient *Ras* activation and the increasing rate of *pR*, respectively (see Supplementary Information, Fig. S5). Red lines in **b** and **c** indicate *Ras* activation with the equivalent parameters in the *in silico* model. (**d**) Simple Rap1 model, in which the pR-dependent GEF activation with constant GAP activity regulates Rap1 activation. (**e**) *Rap1* activation at steady state derived from equation (1), where *pR* is given by a constant, α. (**f**) *Ras* activation at steady state derived from equation (2), where *pR* is given by a constant, α.

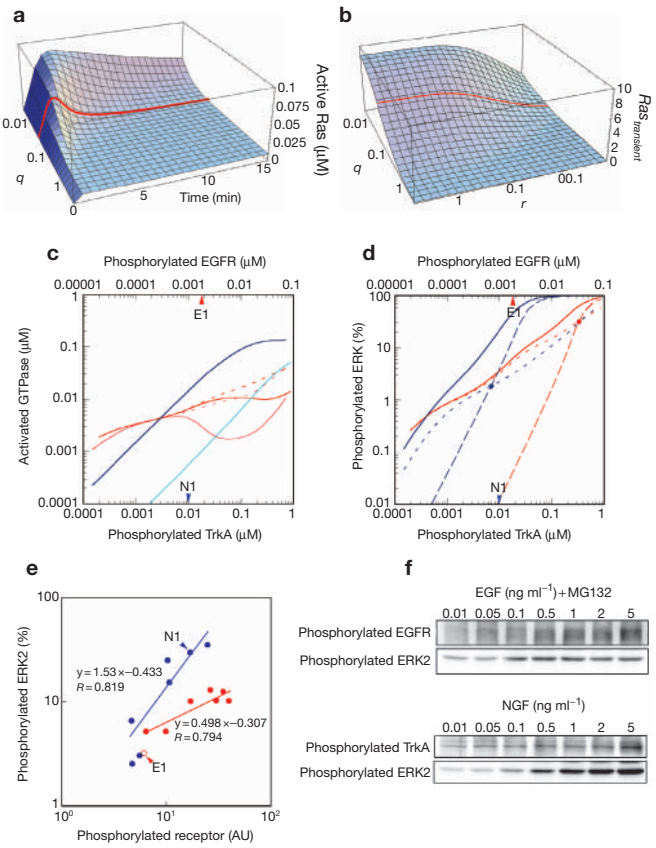

Figure 7 Transient Ras activation, and Ras, Rap1 and ERK activation at steady state. (**a**) A constant phosphorylated epidermal growth-factor receptor (EGFR) stimulus was given, and the *in silico* Ras activation was plotted against the indicated values of *q*. (**b**) $Ras_{transient}$ was plotted against the indicated values of *r* and *q in silico*. Red lines in **a** and **b** indicate Ras activation with the original parameters in the *in silico* model. (**c**) *In silico* Ras and Rap1 activation at steady state against the constant phosphorylated EGFR are shown in red and cyan, and those against the constant phosphorylated TrkA are shown in pink and blue, respectively. Dashed lines indicate Ras activation without negative-feedback inhibition of SOS. (**d**) *In silico* extracellular-signal-regulated kinase (ERK) activation at steady state against the constant phosphorylated EGFR and TrkA are shown with red and blue solid lines, respectively. Dashed and dotted lines indicate Rap1-dependent ERK activation (without Ras activation) and Ras-dependent ERK activation (without Rap1 activation), respectively. Circles indicate the intersecting points of Ras- and Rap1-dependent ERK activation. (**e**) *In vivo* ERK phosphorylation was plotted against phosphorylated EGFR (red) and TrkA (blue) at 30 min. Lines were estimated by the least squares method. (**f**) The corresponding gel images of the results from **e**. Arrowheads in **c**–**e** indicate the points of the phosphorylated receptors induced by 1 ng ml^{-1} of EGF (in the absence of MG-132) and NGF, respectively.

rylated receptors at steady state were also similar at lower doses *in silico* (Fig. 7c). However, the slopes of the plots of Ras activation were lower than those of Rap1 activation at the lower doses, at which GEF and GAP activations were not saturated (Fig. 5a, b). These *in silico* characteristics are consistent with the results in the simple Rap1 and Ras models (Fig. 6e, f), indicating that the simple Rap1 and Ras models also retain essential characteristics of Rap1 and Ras activation at steady state *in silico*. Inhibition of Ras activation at higher doses of both phosphorylated receptors depended on the negative-feedback inhibition of SOS; the deletion of the negative-feedback inhibition of SOS resulted in the disappearance of this inhibition at higher doses without affecting Ras activation at lower doses (Fig. 7c). It is also possible that the negative-feedback inhibition of SOS regulates Ras activation even at lower doses *in vivo*, and further study is necessary to address this issue.

We also predicted the dynamics of ERK activation at steady state against the phosphorylated receptors *in silico*. The slope of the plot of ERK activation versus the phosphorylated EGFR at steady state was lower than that versus the phosphorylated TrkA (Fig. 7d). ERK activation at steady state consisted of Ras- (Fig. 7d, dotted lines) and Rap1- (Fig. 7d, dashed line) dependent ERK activation *in silico*. Ras-dependent ERK activation became dominant at lower doses of the phosphorylated receptors, below the intersecting points (Fig. 7d). In turn, Rap1-dependent ERK activation became dominant at higher doses of the phosphorylated receptors, above the intersecting points (Fig. 7d). The curves of Ras-dependent ERK activation were similar, whereas those of Rap1-dependent ERK activation were different. The distinct Rap1 activation against both phosphorylated receptors is due to the distinct affinities of fibroblast growth factor receptor substrate 2 (FRS2) to both receptors (see below).

We validated the distinct properties of sustained ERK activation *in vivo*. The slope of the plot of the ERK activation versus the phosphorylated EGFR was lower than that versus the phosphorylated TrkA (Fig. 7e, f), which is consistent with the *in silico* prediction.

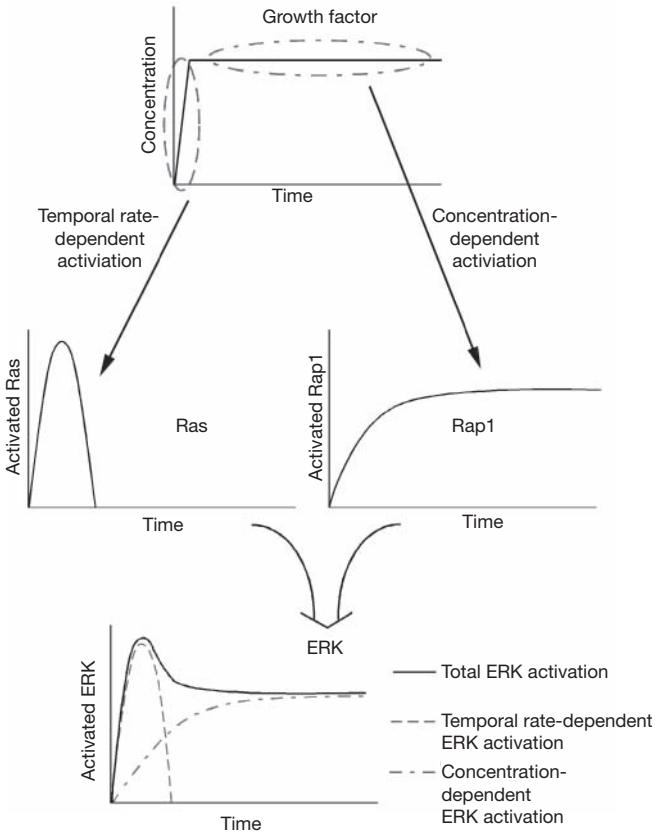

Figure 8 The distinct temporal dynamics of transient and sustained ERK activation via Ras and Rap1 activation. The Ras and Rap1 systems specifically capture the distinct properties of growth factors — the temporal rate and final concentration — and thereby encode these physical properties of growth factors into transient and sustained ERK activation, respectively.

Therefore, these *in silico* and *in vivo* results clearly indicate the distinct dynamics of ERK activation against the phosphorylated EGFR and TrkA at steady state.

DISCUSSION

The crucial difference between EGF- and NGF-dependent ERK activation is the absence or presence of sustained ERK activation, which depends on sustained Rap1 activation. One of the most crucial differences came from the different affinities of FRS2 for the phosphorylated receptors in this model. The affinity of FRS2 for phosphorylated TrkA was higher than that for phosphorylated EGFR (see Supplementary Information, Table S1). Reduction of the affinity of FRS2 for phosphorylated TrkA reduced sustained Rap1 activation (see Supplementary Information, Fig. S3). The amplitude of Rap1 activation in response to NGF became similar to that in response to EGF when the affinities of FRS2 for both phosphorylated receptors were set at 200 nM (see Supplementary Information, Fig. S3j, solid and dashed green lines), indicating that the affinity of FRS2 for the phosphorylated receptor determines the amplitude of Rap1 activation. Another crucial difference was the different dynamics of tyrosine phosphorylation of the receptors. NGF induced sustained tyrosine phosphorylation of TrkA (Fig. 2b), whereas EGF induced transient tyrosine phosphorylation of EGFR due to rapid internalization and degradation (Fig. 2a; also see Supplementary Information, Fig. S3). It should also be noted that, from downstream of the adaptor proteins to ERK, both the topology of the network and the kinetic parameters are identical regardless of the stimuli, indicating that the difference between EGF- and NGF-dependent ERK activation is due to different dynamics upstream of the adaptor proteins.

We showed that the temporal rate and final concentration of growth factors are specifically captured by the Ras and Rap1 systems via transient Ras and sustained Rap1 activation, and then encoded into transient and sustained ERK activation, respectively (Fig. 8). This difference between the Ras and Rap1 systems came from their distinct inactivation processes — slower and constant GAP activity, respectively. This finding also indicates the existence of similar physiological roles of other stimulation-dependent negative regulators[38], such as other GAPs (for example, Rho–GAP), protein tyrosine phosphatases (for example, SHP) and lipid phosphatases (for example, SHIP and PTEN).

We should emphasize that each *in silico* network should be regarded as representative of similar redundant processes, rather than as a complete description. For example, FRS2 is only an adaptor protein for Rap1 activation in the current *in silico* model; however, this protein implicitly represents another adaptor protein, ARMS, which performs a similar function[39]. In conclusion, combining *in silico* and *in vivo* analyses facilitates systematic understanding of the underlying properties of signalling networks.

METHODS

Numerical simulation of biochemical reactions. All reactions were represented by molecule–molecule interactions and enzymatic reactions[23]. We used a *GENESIS* simulator (version 2.2) with a *Kinetikit* interface for solving the ordinary differential equations with a time step of 10 ms[23].

Block diagram and parameters. The model consisted of 22 molecules and 106 rate constants. The rate constants consisted of 70 and 36 rate constants for molecule–molecule interactions and enzymatic reactions, respectively. The biochemical reactions and the rate constants that were used in the study are shown in Supplementary Information, Fig. S1 and Table S1, respectively. The *GENESIS* script of our *in silico* model is also available as a text file on our website (http://www.kurodalab.org/info/ERK.g).

Cell culture and growth-factor treatments. PC12 cells (kindly provided by Masato Nakafuku, Cincinnati Children's Hospital Medical Center, Ohio) (8×10^5) were starved in DMEM for 16 h, then stimulated with the indicated concentrations of NGF (Invitrogen, Carlsbad, CA) or EGF (Roche, Indianapolis, IN). Increasing stimuli of EGF and NGF were added by use of a microsyringe pump (KD Scientific, Holliston, MA) with a continuous 10 µl min^{-1} flow rate into 2 ml of the cultured media.

Immunoblotting. Cell lysates were subjected to standard SDS-PAGE (acrylamide:bis=29.5:1) or low-bis SDS-PAGE (acrylamide:bis=144:1) for the separation of phosphorylated and non-phosphorylated ERK, and then transferred to nitrocellulose membrane. The membranes were probed with anti-phospho EGFR (Y1068) antibody (1:1,000; Cell Signaling Technology, Beverly, MA), anti-phospho TrkA (Y490) antibody (1:1,000; Cell Signaling Technology), anti-SOS1 antibody (1:1,000; Upstate, Charlottesville, VA) or anti-ERK1/2 antibody (1:1,000; Cell Signaling Technology). Anti-phospho ERK1/2 (T202/Y204) antibody (1:1000; Cell Signaling Technology) was used due to its higher sensitivity compared with that of anti-ERK1/2 antibody, and the ratio of phosphorylated to non-phosphorylated ERK2 was estimated by comparison at the same point (5 ng ml^{-1} NGF) using anti-ERK1/2 antibody (Fig. 7f). Horseradish peroxidase (HRP)-conjugated secondary antibodies (Amersham Biosciences, Piscataway, NJ) were used at 1:5,000 and an enhanced chemiluminescence (ECL) detection kit (Amersham Biosciences) was used for HRP detection.

Ras and Rap1 pull-down assay. Ras and Rap1 activation was measured by an affinity pull-down assay using glutathione *S*-transferase (GST)–c-Raf1 (1–149 amino acids) or GST–RalGDS (767–867 amino acids) (kindly provided by Akira Kikuchi, Hiroshima University, Japan) as described elsewhere[40]. The small

GTPases bound to the beads were subjected to SDS-PAGE, followed by immunoblotting with monoclonal anti-Ras (1:500; BD biosciences, Franklin Lakes, NJ) or anti-Rap1 (1:500; BD biosciences) antibodies.

Recruitment of SOS and Ras–GAP to the membrane fractions. PC12 cells were stimulated with a constant rate of 10 ng ml^{-1} EGF, and cells were lysed by sonication at the indicated time with a buffer containing 50 mM Tris-HCl (pH 7.5), 200 mM sucrose, 2.5 mM $MgCl_2$, 10 mM NaF, 1 mM sodium orthovanadate, 1 mM dithiothreitol and 10 μg ml^{-1} leupeptin and aprotinin. After the membrane and cytosol fractions were separated by centrifugation at 100,000 *g* for 30 min, the amounts of SOS and Ras–GAP in both fractions were measured by western blotting.

The simple Ras and Rap1 models. In the simple Ras model in Fig. 6a, the derivatives of pR-GEF and pR-GAP, and GTPase-GTP (Ras or Rap1) are given by:

$$\frac{d[\text{pR-GEF}]}{dt} = k_1[\text{pR}]([\text{GEF}_{\text{Total}}]-[\text{pR-GEF}])-k_2[\text{pR-GEF}] \quad (3)$$

$$\frac{d[\text{pR-GAP}]}{dt} = k_3[\text{pR}]([\text{GAP}_{\text{Total}}]-[\text{pR-GAP}])-k_4[\text{pR-GAP}] \quad (4)$$

$$\frac{d[\text{GTPase-GTP}]}{dt} = k_5[\text{pR-GEF}]([\text{GTPase}_{\text{Total}}]-[\text{GTPase-GTP}]) - k_6[\text{pR-GAP}][\text{GTPase-GTP}] \quad (5)$$

where [ ] denotes the concentration of the molecule at time *t*. The total concentration of GEF, GAP and GTPase ([GEF_{Total}], [GAP_{Total}] and [$GTPase_{Total}$], respectively) are conserved throughout the reactions. Equation (5) implicitly assumes that the concentration of GTPase complexed with either GEF or GAP is relatively small compared with the total concentration of the GTPases, GEF and GAP. We write equations (3) to (5) in dimensionless form, with the following substitutions:

$$\frac{dGEF}{dt} = k_2\{\text{pR}-(1+pR)GEF\} \quad (3')$$

$$\frac{dGAP}{dt} = k_4\{(p\times pR)-(1+(p\times pR))GAP\} \quad (4')$$

$$\frac{dGTPase}{dt} = k_6[\text{GAP}_{\text{Total}}]\{GEF/Ke-(GEF/Ke+GAP)GTPase\} \quad (5')$$

where $pR = [\text{pR}]/Kd$, $GEF = [\text{pR-GEF}]/[\text{GEF}_{\text{Total}}]$, $GAP = [\text{pR-GAP}]/[\text{GAP}_{\text{Total}}]$, *GTPase* (*Ras* or *Rap1*) = [GTPase-GTP]/[$GTPase_{Total}$], $Kd = k_2/k_1 = pk_4/k_3$, $Ke = k_6[GAP_{Total}]/k_5[GEF_{Total}]$. Similarly, $s = k_6[\text{GAP}_{\text{Total}}]/k_2$ represents the relative relaxation time constant of *GTPase* compared with *GEF* where *GEF* and *GAP* are assumed to be constant. In addition, we define $q = k_4/k_2$, which represents the relative rate constant of *GAP* activation compared with *GEF* activation under the conditions in which *pR* is a constant, α, and *GEF* and *GAP* are not saturated (that is, $\alpha << 1$, $p\alpha << 1$) (see Fig. 5 and Supplementary Information Fig. S5, see below). Unless specified, we set $p = 3.5$, $q = 0.027$, $Ke = 3.2$ and $s = 2$ in the simple Ras model (Fig. 6b, c, f) and $Ke = 0.09$ in the simple Rap1 model (Fig. 6e), which are equivalent values in the *in silico* model (data not shown). We also set $\alpha = 0.28$ (Fig. 6b, c), which is equivalent to the concentration of phosphorylated EGFR induced by 1 ng ml^{-1} of EGF in the *in silico* model. The increasing *pR* stimulation is given by $pR = \alpha\{1-\exp(-rk_2t)\}$ where *r* corresponds to the increasing rate of *pR* (Fig. 6c, Supplementary Information, Fig. S5). The relative peak amplitude of the transient *Ras* activation, $Ras_{transient}$, is defined by $Ras_{transient} = (Max-Equi)/Equi$, where *Max* and *Equi* denote *Ras* at the transient peak and steady state, respectively (Fig. 6c, Fig. 7b and Supplementary Information, Fig. S5). The transient *Ras* activation is defined by $Ras_{transient} > 0$ (Fig. 6c, Fig. 7b and Supplementary Information, Fig. S5). The increasing EGF stimuli led to the SOS and RasGAP activation in a dose-dependent manner in EGF (Fig. 5a), indicating that the SOS and GAP activation were not saturated *in silico*. The equivalent conditions in the simple models can be obtained by $\alpha << 1$ and $p\alpha << 1$.

At steady state, the concentrations of the activated *GEF*, *GAP* and *GTPase* become constant. Therefore, by setting the equations (3') to (5') equal to zero, we obtain equation (2). Similarly, we obtain equation (1) from equations (3') and (5'), where *GAP* is always constant ($GAP = 1$). Note that all values in Fig. 6b, c, e, f are dimensionless.

In Fig. 7a, b, we numerically measured the time constants of SOS and RasGAP activation, τ_{SOS} and $\tau_{Ras\text{-}GAP}$, at which time constant EGF stimulation induced 50% of their maximal activation *in silico*, respectively. We defined $q = \tau_{SOS}/\tau_{Ras\text{-}GAP}$, which represents the relative rate constant of the RasGAP activation compared to the SOS activation. Indicated values of *q* were obtained by changing $\tau_{Ras\text{-}GAP}$ without changing τ_{SOS}. For simplicity, the negative feedback inhibition of SOS by ERK was blocked for the analysis in Fig. 7a, b, because the transient Ras activation was not dependent on the negative feedback (Supplementary Information, Fig. S3). We also set [phosphorylated EGFR] = 0.0018 (μM), which corresponds to the phosphorylated EGFR concentration induced by 1 ng ml^{-1} of EGF for constant stimulation (Fig. 7a), and the increasing phosphorylated EGFR stimulus was given by [phosphorylated EGFR] = $0.0018\{1-\exp(-r(t/\tau_{SOS}))\}$ (μM), where *r* corresponds to the increasing rate of phosphorylated EGFR (Fig. 7b).

Supplementary information is available on the Nature Cell Biology website.

ACKNOWLEDGEMENTS

We thank K. Kaibuchi, Y. Gotoh, M. Kawato and M. Arita for critically reading this manuscript, and R. Kettunen and R. Kunihiro for their technical assistance. This work was supported in part by a grant in-aid for scientific research from the Ministry of Education, Culture, Sports, Science and Technology of Japan, and by a grant in-aid from Uehara Memorial Foundation.

COMPETING FINANCIAL INTERESTS

The authors declare that they have no competing financial interests.

Received 15 November 2004; accepted 15 February 2005
Published online at http://www.nature.com/naturecellbiology.

1. Vaudry, D., Stork, P. J., Lazarovici, P. & Eiden, L. E. Signaling pathways for PC12 cell differentiation: making the right connections. *Science* **296,** 1648–1649 (2002).
2. Gotoh, Y. *et al.* Microtubule-associated-protein (MAP) kinase activated by nerve growth factor and epidermal growth factor in PC12 cells. Identity with the mitogen-activated MAP kinase of fibroblastic cells. *Eur. J. Biochem.* **193,** 661–669 (1990).
3. Qiu, M. S. & Green, S. H. PC12 cell neuronal differentiation is associated with prolonged p21ras activity and consequent prolonged ERK activity. *Neuron* **9,** 705–717 (1992).
4. Traverse, S., Gomez, N., Paterson, H., Marshall, C. & Cohen, P. Sustained activation of the mitogen-activated protein (MAP) kinase cascade may be required for differentiation of PC12 cells. Comparison of the effects of nerve growth factor and epidermal growth factor. *Biochem. J.* **288,** 351–355 (1992).
5. Egan, S. E. *et al.* Association of Sos Ras exchange protein with Grb2 is implicated in tyrosine kinase signal transduction and transformation. *Nature* **363,** 45–51 (1993).
6. Rozakis-Adcock, M., Fernley, R., Wade, J., Pawson, T. & Bowtell, D. The SH2 and SH3 domains of mammalian Grb2 couple the EGF receptor to the Ras activator mSos1. *Nature* **363,** 83–85 (1993).
7. Li, N. *et al.* Guanine-nucleotide-releasing factor hSos1 binds to Grb2 and links receptor tyrosine kinases to Ras signalling. *Nature* **363,** 85–88 (1993).
8. Gale, N. W., Kaplan, S., Lowenstein, E. J., Schlessinger, J. & Bar-Sagi, D. Grb2 mediates the EGF-dependent activation of guanine nucleotide exchange on Ras. *Nature* **363,** 88–92 (1993).
9. Davis, R. J. The mitogen-activated protein kinase signal transduction pathway. *J. Biol. Chem.* **268,** 14553–14556 (1993).
10. Di Fiore, P. P. & Gill, G. N. Endocytosis and mitogenic signaling. *Curr. Opin. Cell. Biol.* **11,** 483–488 (1999).
11. Waterman, H. & Yarden, Y. Molecular mechanisms underlying endocytosis and sorting of ErbB receptor tyrosine kinases. *FEBS Lett.* **490,** 142–152 (2001).
12. Soler, C., Beguinot, L., Sorkin, A. & Carpenter, G. Tyrosine phosphorylation of ras GTPase-activating protein does not require association with the epidermal growth factor receptor. *J. Biol. Chem.* **268,** 22010–22019 (1993).
13. Jones, N. & Dumont, D. J. Recruitment of Dok-R to the EGF receptor through its PTB domain is required for attenuation of Erk MAP kinase activation. *Curr. Biol.* **9,** 1057–1060 (1999).
14. Waters, S. B. *et al.* Desensitization of Ras activation by a feedback disassociation of the SOS-Grb2 complex. *J. Biol. Chem.* **270,** 20883–20886 (1995).
15. Dong, C., Waters, S. B., Holt, K. H. & Pessin, J. E. SOS phosphorylation and disassociation of the Grb2–SOS complex by the ERK and JNK signaling pathways. *J. Biol. Chem.* **271,** 6328–6332 (1996).
16. Marshall, C. J. Signal transduction. Taking the Rap. *Nature* **392,** 553–554 (1998).
17. York, R. D. *et al.* Rap1 mediates sustained MAP kinase activation induced by nerve growth factor. *Nature* **392,** 622–666 (1998).
18. Kao, S., Jaiswal, R. K., Kolch, W. & Landreth, G. E. Identification of the mechanisms regulating the differential activation of the MAPK cascade by epidermal growth factor and nerve growth factor in PC12 cells. *J. Biol. Chem.* **276,** 18169–18177 (2001).
19. Wu, C., Lai, C. F. & Mobley, W. C. Nerve growth factor activates persistent Rap1 signaling in endosomes. *J. Neurosci.* **21,** 5406–5416 (2001).

20. Chang, J. H., Mellon, E., Schanen, N. C. & Twiss, J. L. Persistent TrkA activity is necessary to maintain transcription in neuronally differentiated PC12 cells. *J. Biol. Chem.* **278,** 42877–42885 (2003).
21. Ohtsuka, T., Shimizu, K., Yamamori, B., Kuroda, S. & Takai, Y. Activation of brain B-Raf protein kinase by Rap1B small GTP-binding protein. *J. Biol. Chem.* **271,** 1258–1261 (1996).
22. Vossler, M. R. *et al.* cAMP activates MAP kinase and Elk-1 through a B-Raf- and Rap1-dependent pathway. *Cell* **89,** 73–82 (1997).
23. Bhalla, U. S. & Iyengar, R. Emergent properties of networks of biological signaling pathways. *Science* **283,** 381–387 (1999).
24. Schoeberl, B., Eichler-Jonsson, C., Gilles, E. D. & Muller, G. Computational modeling of the dynamics of the MAP kinase cascade activated by surface and internalized EGF receptors. *Nature Biotechnol.* **20,** 370–375 (2002).
25. Brightman, F. A. & Fell, D. A. Differential feedback regulation of the MAPK cascade underlies the quantitative differences in EGF and NGF signalling in PC12 cells. *FEBS Lett.* **482,** 169–174 (2000).
26. Shvartsman, S. Y. *et al.* Autocrine loops with positive feedback enable context-dependent cell signaling. *Am. J. Physiol. Cell. Physiol.* **282,** C545–C559 (2002).
27. Bhalla, U. S., Ram, P. T. & Iyengar, R. MAP kinase phosphatase as a locus of flexibility in a mitogen-activated protein kinase signaling network. *Science* **297,** 1018–1023 (2002).
28. Hatakeyama, M. *et al.* A computational model on the modulation of mitogen-activated protein kinase (MAPK) and Akt pathways in heregulin-induced ErbB signalling. *Biochem. J.* **373,** 451–463 (2003).
29. Yamada, S., Taketomi, T. & Yoshimura, A. Model analysis of difference between EGF pathway and FGF pathway. *Biochem. Biophys. Res. Commun.* **314,** 1113–1120 (2004).
30. Kholodenko, B. N., Demin, O. V., Moehren, G. & Hoek, J. B. Quantification of short term signaling by the epidermal growth factor receptor. *J. Biol. Chem.* **274,** 30169–30181 (1999).
31. Downward, J. The GRB2/Sem-5 adaptor protein. *FEBS Lett.* **338,** 113–117 (1994).
32. Langlois, W. J., Sasaoka, T., Saltiel, A. R. & Olefsky, J. M. Negative feedback regulation and desensitization of insulin- and epidermal growth factor-stimulated p21ras activation. *J. Biol. Chem.* **270,** 25320–25323 (1995).
33. Holt, K. H. *et al.* Epidermal growth factor receptor targeting prevents uncoupling of the Grb2-SOS complex. *J. Biol. Chem.* **271,** 8300–8306 (1996).
34. Nishida, E. & Gotoh, Y. The MAP kinase cascade is essential for diverse signal transduction pathways. *Trends Biochem. Sci.* **18,** 128–131 (1993).
35. Bourne, H. R., Sanders, D. A. & McCormick, F. The GTPase superfamily: conserved structure and molecular mechanism. *Nature* **349,** 117–127 (1991).
36. Choi, D. Y., Toledo-Aral, J. J., Segal, R. & Halegoua, S. Sustained signaling by phospholipase C-gamma mediates nerve growth factor-triggered gene expression. *Mol. Cell. Biol.* **21,** 2695–2705 (2001).
37. Longva, K. E. *et al.* Ubiquitination and proteasomal activity is required for transport of the EGF receptor to inner membranes of multivesicular bodies. *J. Cell Biol.* **156,** 843–854 (2002).
38. Moghal, N. & Sternberg, P. W. Multiple positive and negative regulators of signaling by the EGF-receptor. *Curr. Opin. Cell Biol.* **11,** 190–196 (1999).
39. Arevalo, J. C., Yano, H., Teng, K. K. & Chao, M. V. A unique pathway for sustained neurotrophin signaling through an ankyrin-rich membrane-spanning protein. *EMBO J.* **23,** 2358–2368 (2004).
40. de Rooij, J. & Bos, J. L. Minimal Ras-binding domain of Raf1 can be used as an activation-specific probe for Ras. *Oncogene* **14,** 623–625 (1997).

a

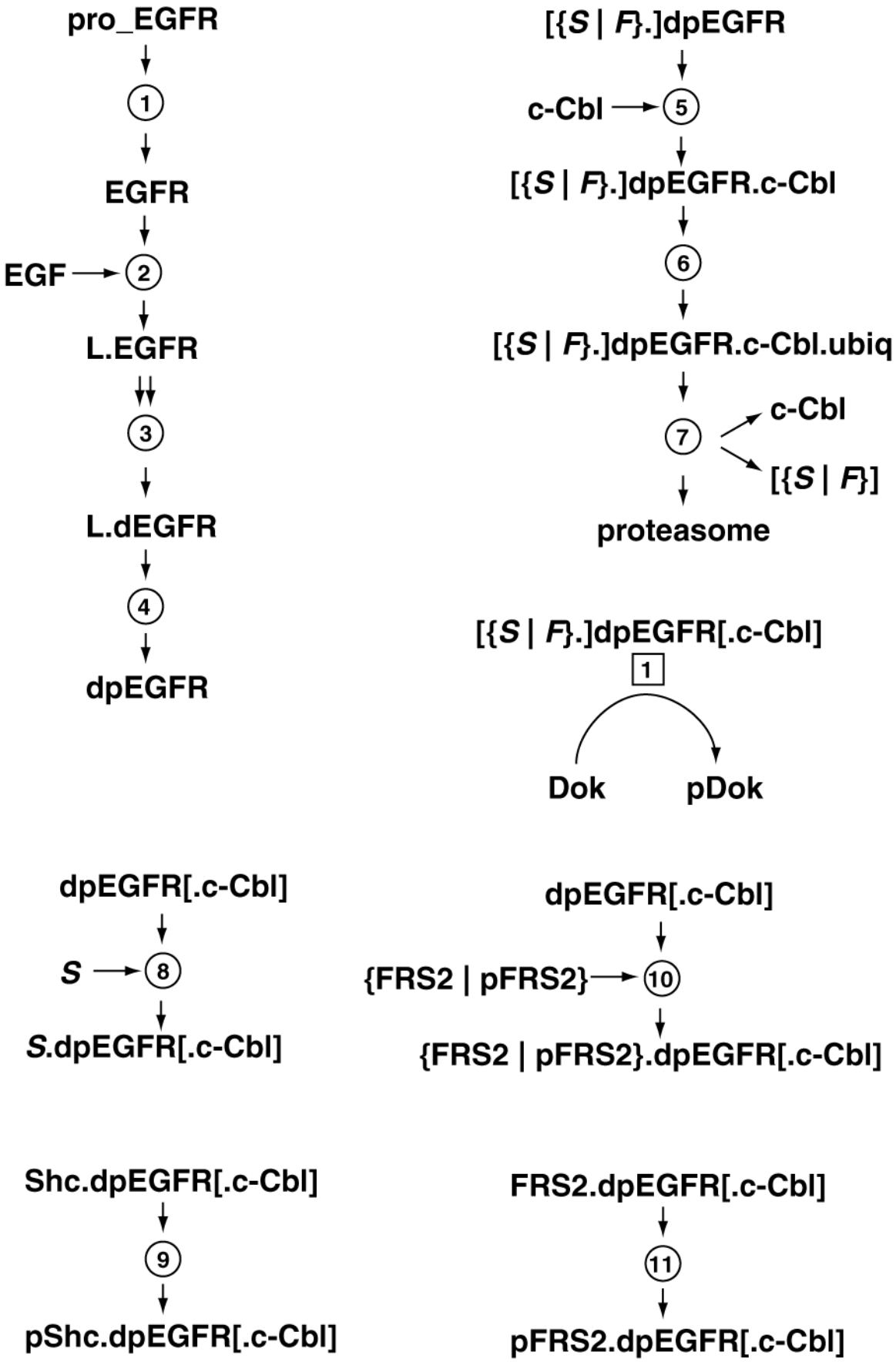

S and ***F*** denote **{Shc | [Grb2.SOS.]pShc}** and **{FRS2 | [Crk.C3G.]pFRS2}**, respectively.

Kuroda_Fig. S1a

b

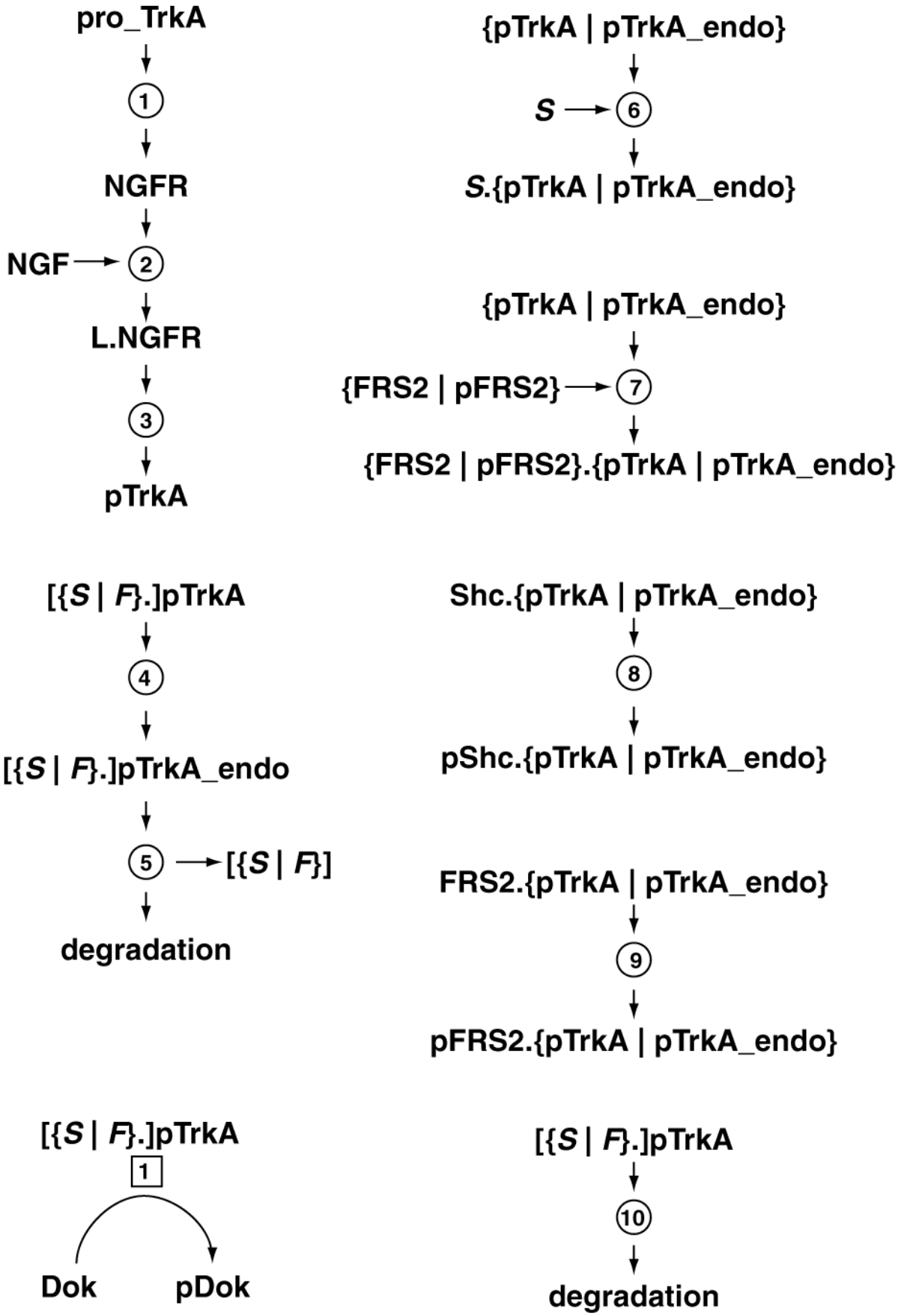

S and ***F*** denote **{Shc | [Grb2.SOS.]pShc}** and **{FRS2 | [Crk.C3G.]pFRS2}**, respectively.

Kuroda_Fig. S1b

c

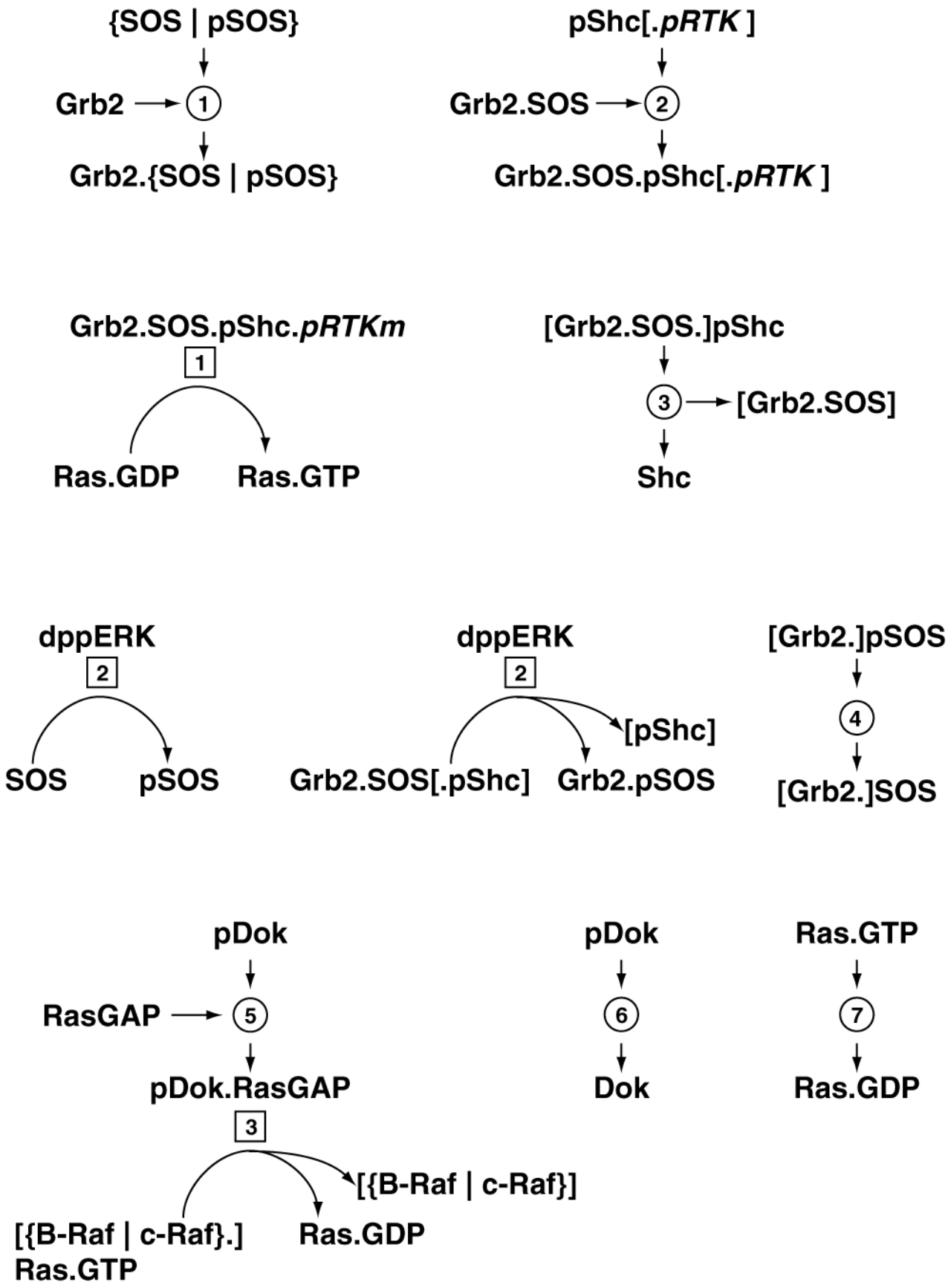

pRTKm and ***pRTK*** denote **{dpEGFR[.c-Cbl] | pTrkA}** and **{dpEGFR[.c-Cbl] | pTrkA | pTrkA_endo}**, respectively.

Kuroda_Fig. S1c

d

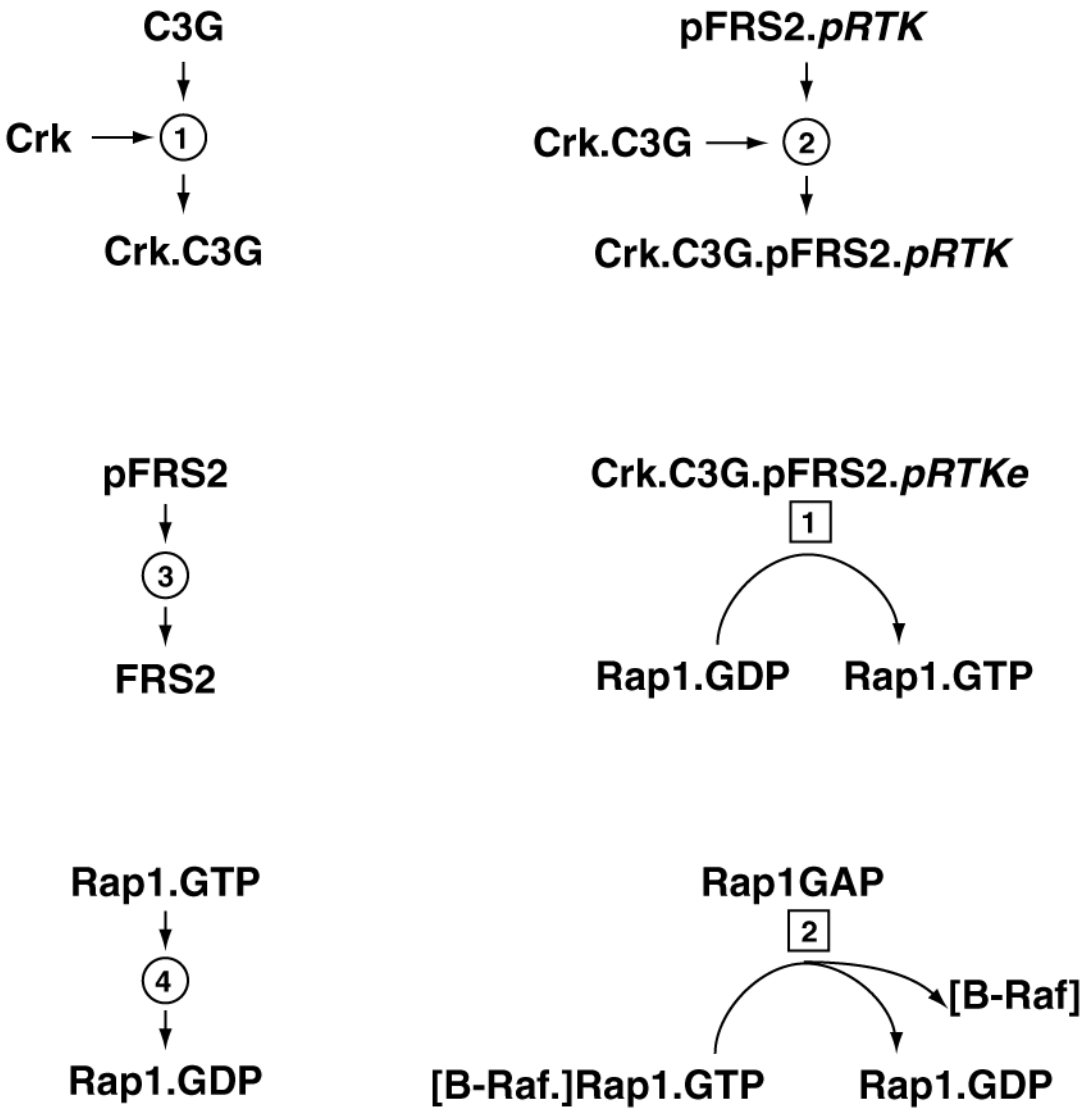

pRTKe and ***pRTK*** denote **{dpEGFR[.c-Cbl] | pTrkA_endo}** and **{dpEGFR[.c-Cbl] | pTrkA | pTrkA_endo}**, respectively.

Kuroda_Fig. S1d

e

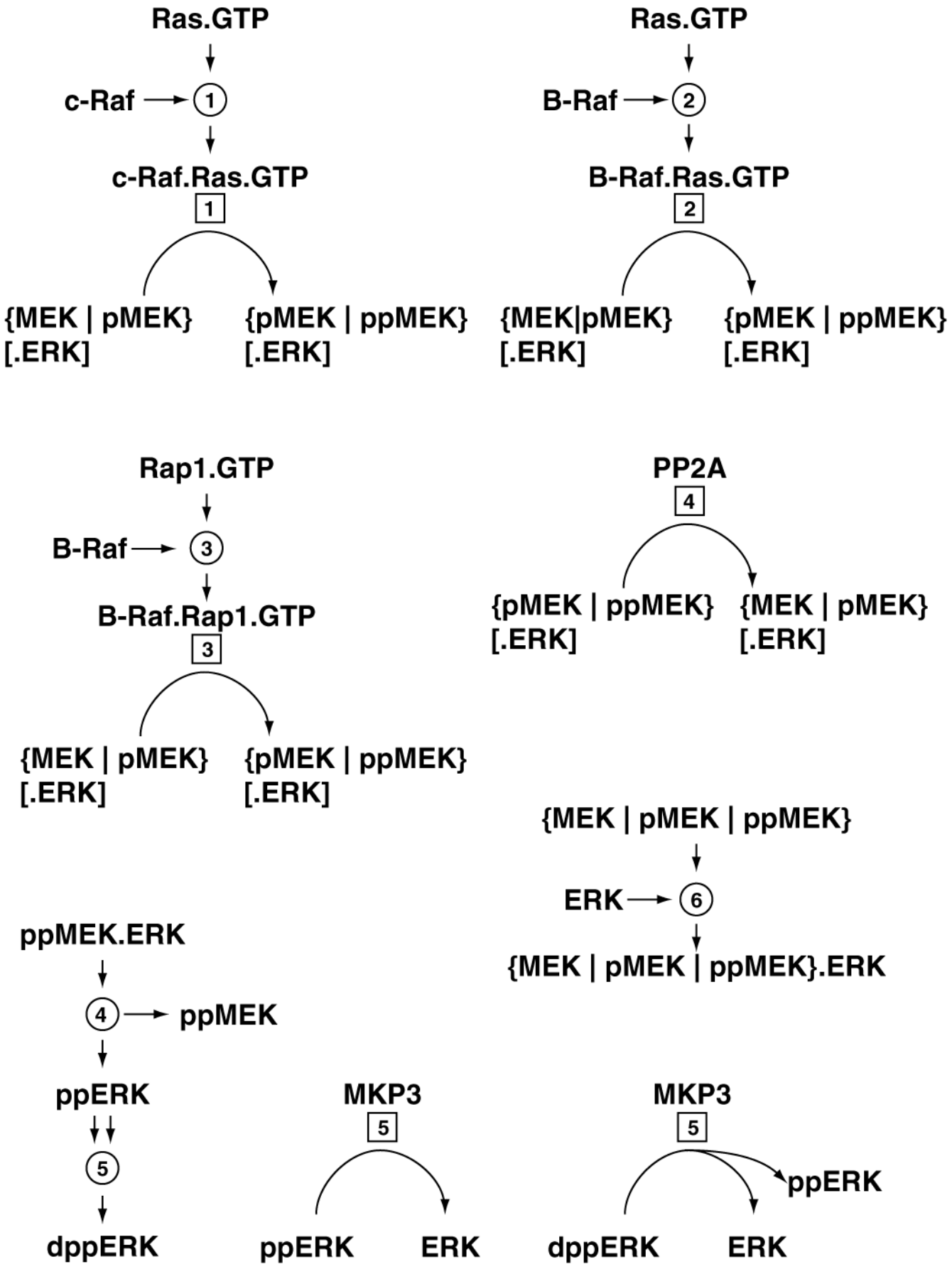

Kuroda_Fig. S1e

Notation of Figure S1

Circles with arrows denote molecule-molecule interactions. Boxes with round arrows denote enzymatic reactions. Rate constants (Numbered circles or boxes) and concentrations of molecules are shown in Supplementary Information, Table S1. Periods between molecules denote non-covalent binding. p and pp denote monophosphorylated and diphosphorylated molecules, respectively. d denotes a dimerised molecule. [ ] denotes an optional component(s) of the complex which shares the same kinetic parameters. For example, [pShc.[Sos.Grb2.]]pEGFR indicates either pEGFR alone, pShc.pEGFR, or pShc.Sos.Grb2.pEGFR. { | } denotes an exclusive component which shares the same kinetic parameters. For example, {SOS|pSOS} indicates either SOS or pSOS.

Figure S1a Tyrosine phosphorylation of EGFR and recruitment of adaptor proteins to EGFR. Binding of EGF to EGFR triggers the dimerisation of the receptors, resulting in autophosphorylation of the receptors[1]. Phosphorylated EGFR binds adaptor proteins including Shc[2], c-Cbl[3,4] and FRS2[5], and phosphorylates these adaptor proteins and Dok[6]. EGFR complexed with c-Cbl is ubiquitinated and degraded by proteasome[7-9]. *S* and *F* denote {Shc | [Grb2.Sos.]pShc} and {FRS2 | [Crk.C3G.]pFRS2}, respectively.

Figure S1b Tyrosine phosphorylation of TrkA and recruitment of adaptor proteins to TrkA. Binding of NGF to NGFR, consisting of TrkA and p75, triggers autophosphorylation of TrkA[10]. Phosphorylated TrkA binds adaptor proteins including Shc[11,12] and FRS2[13-15], and phosphorylates the adaptor proteins and Dok. Because the binding of Shc and FRS2 to TrkA compete[14,15], Shc and FRS2 exclusively bind TrkA in this model. Activated TrkA complexed with adaptor proteins is internalised to endosome where Rap1 is activated[16]. Internalisation of TrkA in this model is

represented as a single exponetial decay, however, this implicitly represents the PI-3 kinase dependent internalisation of the TrkA[17]. *S* and *F* denote {Shc | [Grb2.Sos.]pShc} and {FRS2 | [Crk.C3G.]pFRS2}, respectively.

Figure S1c Activation of Ras. Grb2 and SOS complex[18-23] is recruited to phosphorylated Shc bound to EGFR[2] or TrkA[11,12] and catalyse GDP/GTP exchange reaction of Ras[18-23]. Activated ERK phosphorylates SOS[24,25] and phosphorylated SOS dissociates from the complex with Shc[26,27]. Sprouty[28,29] and Spred[30] have recently been shown to be involved in negative feedback inhibition of Ras. In this model, ERK-dependent negative feedback inhibition of SOS implicitly represents Sprouty-dependent negative feedback inhibition because these pathways can be computationally regarded as similar pathways. RasGAP recruited to phosphorylated Dok[6] facilitates intrinsic GTPase reaction of Ras[31]. Ras.GTP is also inactivated by intrinsic GTPase activity[31]. *pRTKm* and *pRTK* denote {dpEGFR[.c-Cbl] | pTrkA} and {dpEGFR[.c-Cbl] | pTrkA | pTrkA _endo}, respectively.

Figure S1d Activation of Rap1. Crk and C3G complex[32] is recruited to phosphorylated FRS2 bound to the receptors[14,33], and catalyse GDP/GTP exchange reaction of Rap1[34]. Rap1GAP facilitates intrinsic GTPase activity of Rap1[35]. Rap1.GTP is also inactivated by its intrinsic GTPase activity[31]. Recruitment of Crk and C3G complex to TrkA may involve other adaptor proteins including SHP[16,36], Gab2[16] and p130CAS[16,37]. In this model, FRS2-dependent recruitment of Crk and C3G complex to TrkA implicitly represents these similar pathways. *pRTKe* and *pRTK* denote {dpEGFR[.c-Cbl] | pTrkA_endo} and {dpEGFR[.c-Cbl] | pTrkA | pTrkA _endo}, respectively.

Figure S1e Activation of Raf, MEK and ERK. GTP-bound forms of Ras and Rap1 interact with c-Raf[38-43] and B-Raf[44-46], and B-Raf[47,48], respectively, and activated c-Raf and B-Raf phosphorylate MEK. Phosphorylation of MEK at S218 and S222 (rat MEK1) results in activation of MEK[49-51]. Phosphorylated MEK is dephosphorylated by PP2A[52-55]. Unphosphorylated ERK forms complex with MEK[56,57]. Activated MEK phosphorylates ERK at T183 and Y185 (rat ERK2) and this dual phosphorylation leads to activation[58,59] release from the complex with MEK[60], and dimerisation[61] of ERK. Phosphorylated ERK is dephosphorylated by MKP3[62,63].

References

1. Schlessinger, J. Ligand-induced, receptor-mediated dimerization and activation of EGF receptor. *Cell* **110**, 669-672 (2002).
2. Rozakis-Adcock, M. *et al.* Association of the Shc and Grb2/Sem5 SH2-containing proteins is implicated in activation of the Ras pathway by tyrosine kinases. *Nature* **360**, 689-692 (1992).
3. Tanaka, S., Neff, L., Baron, R. & Levy, J. B. Tyrosine phosphorylation and translocation of the c-cbl protein after activation of tyrosine kinase signaling pathways. *J. Biol. Chem.* **270**, 14347-14351 (1995).
4. Galisteo, M. L., Dikic, I., Batzer, A. G., Langdon, W. Y. & Schlessinger, J. Tyrosine phosphorylation of the c-cbl proto-oncogene protein product and association with epidermal growth factor (EGF) receptor upon EGF stimulation. *J. Biol. Chem.* **270**, 20242-20245 (1995).
5. Wu, Y., Chen, Z. & Ullrich, A. EGFR and FGFR signaling through FRS2 is subject to negative feedback control by ERK1/2. *Biol. Chem.* **384**, 1215-1226 (2003).
6. Jones, N. & Dumont, D. J. Recruitment of Dok-R to the EGF receptor through its PTB domain is required for attenuation of Erk MAP kinase activation. *Curr. Biol.* **9**, 1057-1060 (1999).
7. Levkowitz, G. *et al.* c-Cbl/Sli-1 regulates endocytic sorting and ubiquitination of the epidermal growth factor receptor. *Genes Dev.* **12**, 3663-3674 (1998).
8. Waterman, H. & Yarden, Y. Molecular mechanisms underlying endocytosis and sorting of ErbB receptor tyrosine kinases. *FEBS Lett.* **490**, 142-152 (2001).
9. Di Fiore, P. P. & Gill, G. N. Endocytosis and mitogenic signaling. *Curr. Opin. Cell. Biol.* **11**, 483-488 (1999).
10. Kaplan, D. R. & Miller, F. D. Signal transduction by the neurotrophin receptors. *Curr. Opin. Cell Biol.* **9**, 213-221 (1997).

11. Obermeier, A. *et al.* Neuronal differentiation signals are controlled by nerve growth factor receptor/Trk binding sites for SHC and PLC gamma. *EMBO J.* **13**, 1585-1590 (1994).
12. Stephens, R. M. *et al.* Trk receptors use redundant signal transduction pathways involving SHC and PLC-gamma 1 to mediate NGF responses. *Neuron* **12**, 691-705 (1994).
13. Kouhara, H. *et al.* A lipid-anchored Grb2-binding protein that links FGF-receptor activation to the Ras/MAPK signaling pathway. *Cell* **89**, 693-702 (1997).
14. Meakin, S. O., MacDonald, J. I., Gryz, E. A., Kubu, C. J. & Verdi, J. M. The signaling adapter FRS-2 competes with Shc for binding to the nerve growth factor receptor TrkA. A model for discriminating proliferation and differentiation. *J. Biol. Chem.* **274**, 9861-9870 (1999).
15. Ong, S. H. *et al.* FRS2 proteins recruit intracellular signaling pathways by binding to diverse targets on fibroblast growth factor and nerve growth factor receptors. *Mol. Cell. Biol.* **20**, 979-989 (2000).
16. Wu, C., Lai, C. F. & Mobley, W. C. Nerve growth factor activates persistent Rap1 signaling in endosomes. *J. Neurosci.* **21**, 5406-54016 (2001).
17. York, R. D. *et al.* Role of phosphoinositide 3-kinase and endocytosis in nerve growth factor-induced extracellular signal-regulated kinase activation via Ras and Rap1. *Mol. Cell. Biol.* **20**, 8069-8083 (2000).
18. Egan, S. E. *et al.* Association of Sos Ras exchange protein with Grb2 is implicated in tyrosine kinase signal transduction and transformation. *Nature* **363**, 45-51 (1993).
19. Rozakis-Adcock, M., Fernley, R., Wade, J., Pawson, T. & Bowtell, D. The SH2 and SH3 domains of mammalian Grb2 couple the EGF receptor to the Ras activator mSos1. *Nature* **363**, 83-85 (1993).
20. Li, N. *et al.* Guanine-nucleotide-releasing factor hSos1 binds to Grb2 and links receptor tyrosine kinases to Ras signalling. *Nature* **363**, 85-88 (1993).
21. Gale, N. W., Kaplan, S., Lowenstein, E. J., Schlessinger, J. & Bar-Sagi, D. Grb2 mediates the EGF-dependent activation of guanine nucleotide exchange on Ras. *Nature* **363**, 88-92 (1993).
22. Buday, L. & Downward, J. Epidermal growth factor regulates p21ras through the formation of a complex of receptor, Grb2 adapter protein, and Sos nucleotide exchange factor. *Cell* **73**, 611-20 (1993).
23. Chardin, P. *et al.* Human Sos1: a guanine nucleotide exchange factor for Ras that binds to GRB2. *Science* **260**, 1338-1343 (1993).
24. Langlois, W. J., Sasaoka, T., Saltiel, A. R. & Olefsky, J. M. Negative feedback regulation and desensitization of insulin- and epidermal growth factor-stimulated p21ras activation. *J. Biol. Chem.* **270**, 25320-25323 (1995).
25. Waters, S. B. *et al.* Desensitization of Ras activation by a feedback disassociation of the SOS-Grb2 complex. *J. Biol. Chem.* **270**, 20883-20886 (1995).
26. Holt, K. H. *et al.* Epidermal growth factor receptor targeting prevents uncoupling of the Grb2-SOS complex. *J. Biol. Chem.* **271**, 8300-8306 (1996).
27. Waters, S. B. *et al.* Insulin and epidermal growth factor receptors regulate distinct pools of Grb2-SOS in the control of Ras activation. *J. Biol. Chem.* **271**, 18224-18230 (1996).

28. Gross, I., Bassit, B., Benezra, M. & Licht, J. D. Mammalian sprouty proteins inhibit cell growth and differentiation by preventing ras activation. *J. Biol. Chem.* **276**, 46460-46468 (2001).
29. Hanafusa, H., Torii, S., Yasunaga, T. & Nishida, E. Sprouty1 and Sprouty2 provide a control mechanism for the Ras/MAPK signalling pathway. *Nat. Cell Biol.* **4**, 850-858 (2002).
30. Wakioka, T. *et al.* Spred is a Sprouty-related suppressor of Ras signalling. *Nature* **412**, 647-651 (2001).
31. Bourne, H. R., Sanders, D. A. & McCormick, F. The GTPase superfamily: conserved structure and molecular mechanism. *Nature* **349**, 117-127 (1991).
32. Tanaka, S. *et al.* C3G, a guanine nucleotide-releasing protein expressed ubiquitously, binds to the Src homology 3 domains of CRK and GRB2/ASH proteins. *Proc. Natl. Acad. Sci. U.S.A.* **91**, 3443-3447 (1994).
33. Kao, S., Jaiswal, R. K., Kolch, W. & Landreth, G. E. Identification of the mechanisms regulating the differential activation of the mapk cascade by epidermal growth factor and nerve growth factor in PC12 cells. *J. Biol. Chem.* **276**, 18169-18177 (2001).
34. Matsuda, M. *et al.* CRK protein binds to two guanine nucleotide-releasing proteins for the Ras family and modulates nerve growth factor-induced activation of Ras in PC12 cells. *Mol. Cell. Biol.* **14**, 5495-5500 (1994).
35. Rubinfeld, B. *et al.* Molecular cloning of a GTPase activating protein specific for the Krev-1 protein p21rap1. *Cell* **65**, 1033-1042 (1991).
36. Hadari, Y. R., Kouhara, H., Lax, I. & Schlessinger, J. Binding of Shp2 tyrosine phosphatase to FRS2 is essential for fibroblast growth factor-induced PC12 cell differentiation. *Mol. Cell. Biol.* **18**, 3966-3973 (1998).
37. Sakai, R. *et al.* A novel signaling molecule, p130, forms stable complexes in vivo with v-Crk and v-Src in a tyrosine phosphorylation-dependent manner. *EMBO J.* **13**, 3748-3756 (1994).
38. Moodie, S. A., Willumsen, B. M., Weber, M. J. & Wolfman, A. Complexes of Ras.GTP with Raf-1 and mitogen-activated protein kinase kinase. *Science* **260**, 1658-1661 (1993).
39. Zhang, X. F. *et al.* Normal and oncogenic p21ras proteins bind to the amino-terminal regulatory domain of c-Raf-1. *Nature* **364**, 308-313 (1993).
40. Warne, P. H., Viciana, P. R. & Downward, J. Direct interaction of Ras and the amino-terminal region of Raf-1 in vitro. *Nature* **364**, 352-355 (1993).
41. Van Aelst, L., Barr, M., Marcus, S., Polverino, A. & Wigler, M. Complex formation between RAS and RAF and other protein kinases. *Proc. Natl. Acad. Sci. U.S.A.* **90**, 6213-6217 (1993).
42. Vojtek, A. B., Hollenberg, S. M. & Cooper, J. A. Mammalian Ras interacts directly with the serine/threonine kinase Raf. *Cell* **74**, 205-214 (1993).
43. Koide, H., Satoh, T., Nakafuku, M. & Kaziro, Y. GTP-dependent association of Raf-1 with Ha-Ras: identification of Raf as a target downstream of Ras in mammalian cells. *Proc. Natl. Acad. Sci. U.S.A.* **90**, 8683-8686 (1993).
44. Jaiswal, R. K., Moodie, S. A., Wolfman, A. & Landreth, G. E. The mitogen-activated protein kinase cascade is activated by B-Raf in response to nerve growth factor through interaction with p21ras. *Mol. Cell. Biol.* **14**, 6944-6953 (1994).

45. Moodie, S. A., Paris, M. J., Kolch, W. & Wolfman, A. Association of MEK1 with p21ras.GMPPNP is dependent on B-Raf. *Mol. Cell. Biol.* **14**, 7153-7162 (1994).
46. Yamamori, B. *et al.* Purification of a Ras-dependent mitogen-activated protein kinase kinase kinase from bovine brain cytosol and its identification as a complex of B-Raf and 14-3-3 proteins. *J. Biol. Chem.* **270**, 11723-11726 (1995).
47. Ohtsuka, T., Shimizu, K., Yamamori, B., Kuroda, S. & Takai, Y. Activation of brain B-Raf protein kinase by Rap1B small GTP-binding protein. *J. Biol. Chem.* **271**, 1258-1261 (1996).
48. Vossler, M. R. *et al.* cAMP activates MAP kinase and Elk-1 through a B-Raf- and Rap1-dependent pathway. *Cell* **89**, 73-82 (1997).
49. Alessi, D. R. *et al.* Identification of the sites in MAP kinase kinase-1 phosphorylated by p74raf-1. *EMBO J.* **13**, 1610-1619 (1994).
50. Cowley, S., Paterson, H., Kemp, P. & Marshall, C. J. Activation of MAP kinase kinase is necessary and sufficient for PC12 differentiation and for transformation of NIH 3T3 cells. *Cell* **77**, 841-852 (1994).
51. Zheng, C. F. & Guan, K. L. Activation of MEK family kinases requires phosphorylation of two conserved Ser/Thr residues. *EMBO J.* **13**, 1123-1131 (1994).
52. Gomez, N. & Cohen, P. Dissection of the protein kinase cascade by which nerve growth factor activates MAP kinases. *Nature* **353**, 170-173 (1991).
53. Shirakabe, K., Gotoh, Y. & Nishida, E. A mitogen-activated protein (MAP) kinase activating factor in mammalian mitogen-stimulated cells is homologous to Xenopus M phase MAP kinase activator. *J. Biol. Chem.* **267**, 16685-16690 (1992).
54. Seger, R. *et al.* Purification and characterization of mitogen-activated protein kinase activator(s) from epidermal growth factor-stimulated A431 cells. *J. Biol. Chem.* **267**, 14373-14381 (1992).
55. Crews, C. M. & Erikson, R. L. Purification of a murine protein-tyrosine/threonine kinase that phosphorylates and activates the Erk-1 gene product: relationship to the fission yeast byr1 gene product. *Proc. Natl. Acad. Sci. U.S.A.* **89**, 8205-8209 (1992).
56. Fukuda, M., Gotoh, Y. & Nishida, E. Interaction of MAP kinase with MAP kinase kinase: its possible role in the control of nucleocytoplasmic transport of MAP kinase. *EMBO J.* **16**, 1901-1908 (1997).
57. Rubinfeld, H., Hanoch, T. & Seger, R. Identification of a cytoplasmic-retention sequence in ERK2. *J. Biol. Chem.* **274**, 30349-30352 (1999).
58. Davis, R. J. The mitogen-activated protein kinase signal transduction pathway. *J. Biol. Chem.* **268**, 14553-14556 (1993).
59. Nishida, E. & Gotoh, Y. The MAP kinase cascade is essential for diverse signal transduction pathways. *Trends Biochem. Sci.* **18**, 128-131 (1993).
60. Adachi, M., Fukuda, M. & Nishida, E. Two co-existing mechanisms for nuclear import of MAP kinase: passive diffusion of a monomer and active transport of a dimer. *EMBO J.* **18**, 5347-5358 (1999).
61. Khokhlatchev, A. V. *et al.* Phosphorylation of the MAP kinase ERK2 promotes its homodimerization and nuclear translocation. *Cell* **93**, 605-615 (1998).

62. Zhao, Y. & Zhang, Z. Y. The mechanism of dephosphorylation of extracellular signal-regulated kinase 2 by mitogen-activated protein kinase phosphatase 3. *J. Biol. Chem.* **276**, 32382-32391 (2001).
63. Farooq, A. & Zhou, M. M. Structure and regulation of MAPK phosphatases. *Cell. Signal.* **16**, 769-779 (2004).

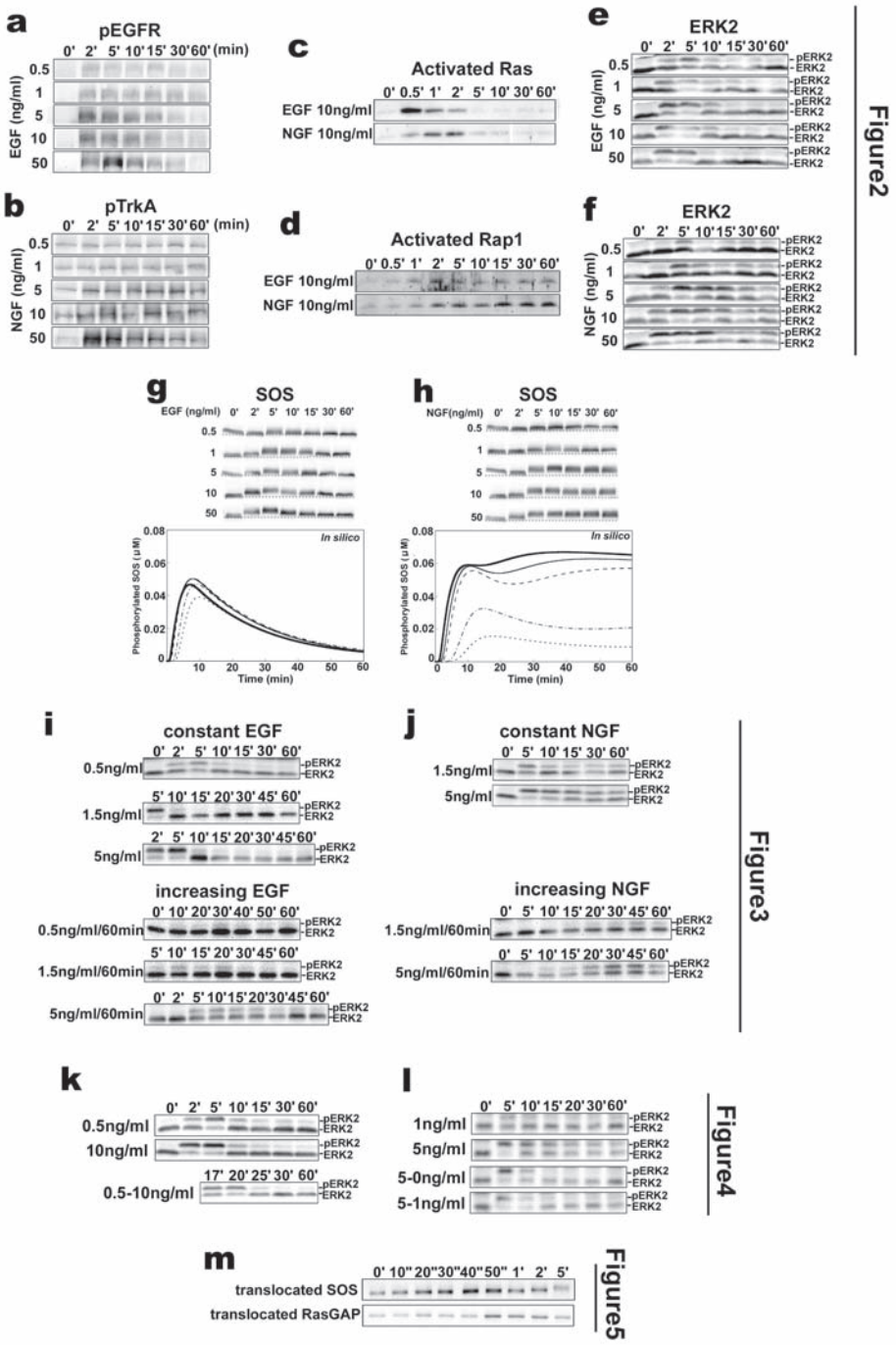

Figure S2 Images of the original gels in Fig. 1, Fig. 2, Fig. 3 and Fig. 4. (a) phosphorylated EGFR at Y1068 (pEGFR) (Fig. 2a), (b) phosphorylated TrkA at Y490 (pTrkA) (Fig. 2b), (c) activated Ras (Fig. 2c), (d) activated Rap1 (Fig. 2d), (e) EGF-induced phosphorylated and nonphosphorylated ERK2 (pERK2 and ERK2) (Fig. 2e), (f) NGF-induced phosphorylated and nonphosphorylated ERK2 (Fig. 2f), (g) EGF-induced SOS mobility shift in vivo (upper panel) and in silico (lower panel), (h) NGF-induced SOS mobility shift in vivo (upper panel) and in silico (lower panel), (i) constant and increasing EGF stimuli-induced ERK2 activation (Fig. 3a), (j) constant and increasing NGF stimuli-induced ERK2 activation (Fig. 3b), (k) a stepwise increase of EGF stimuli-induced ERK2 activation (Fig. 4a), (l) a stepwise decrease of NGF stimuli-induced ERK2 activation (Fig. 4b), and (m) constant EGF stimuli-induced SOS and Ras GAP recruitment to the membrane fractions (Fig. 5c). Since the temporal patterns of phosphorylated ERK1 and ERK2 were always similar (data not shown), phosphorylated ERK2 per total ERK2 were plotted for all figures.

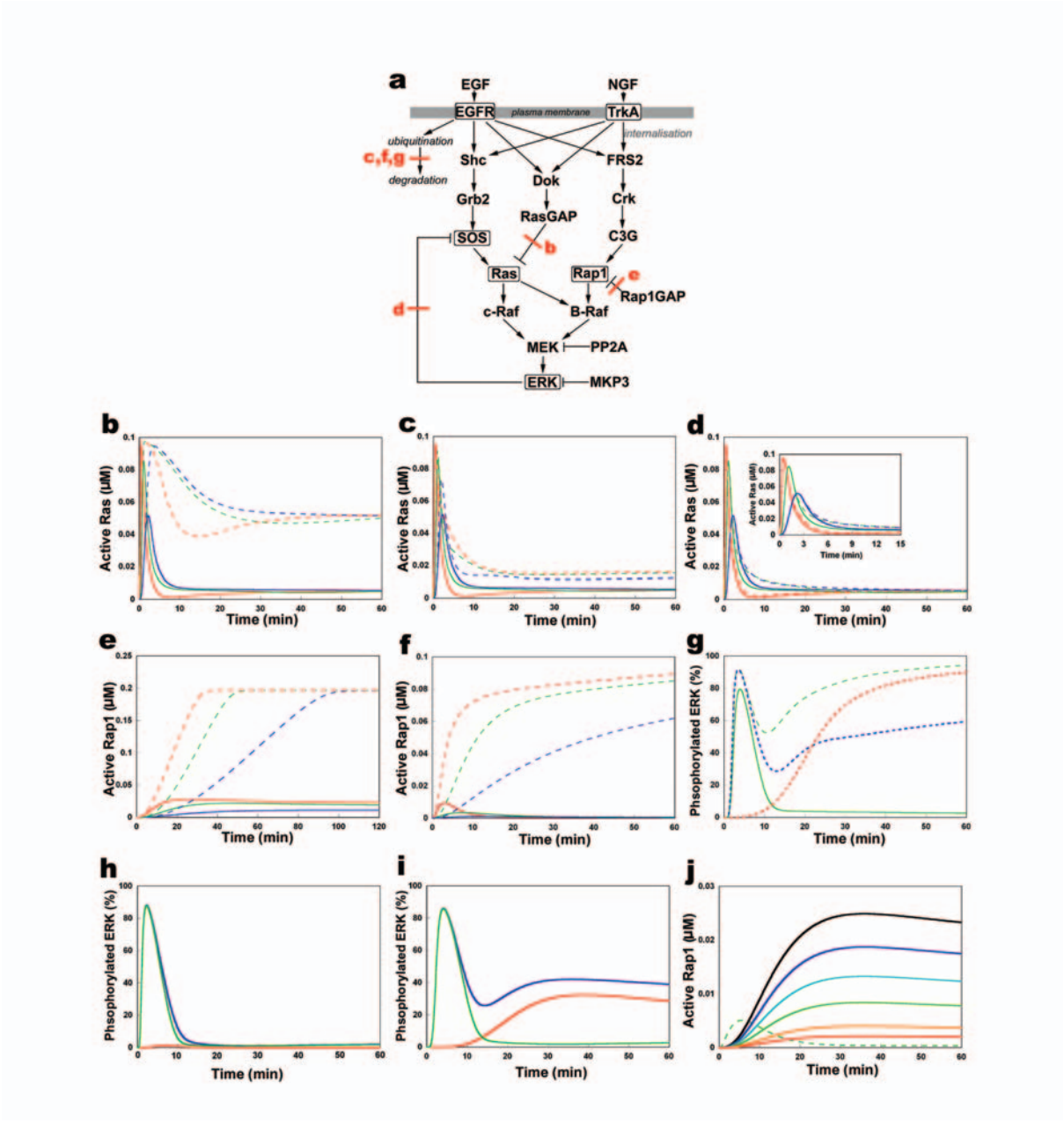

Figure S3 In silico roles of molecules in Ras, Rap1 and ERK activation. Roles of the indicated molecules in Ras and Rap1 activation in silico (a-g). (a) The pathway indicated by a red bar was blocked and Ras and Rap1 activations were plotted as follows. Constant EGF stimuli were given in the presence or absence of either RasGAP (b), EGFR internalisation (c, f) and ERK-dependent feedback inhibition of SOS (d), and Ras activation (b-d) and Rap1 activation (f) were plotted. Solid line, normal conditions; dashed line, in the absence of the indicated pathway. The inset in d is the transient Ras activation within 15 min after stimulation. (e) Constant NGF stimuli were given in the presence or absence of Rap1GAP, and Rap1 activation was plotted. Red, green and blue lines indicate the ERK phosphorylation with constant 50, 5 or 1 ng/ml of either EGF or NGF stimuli, respectively. (g) Constant EGF stimulus (1 ng/ml) was given in the presence or absence of EGFR internalisation, the Ras or the Rap1 activation, and the ERK activation were plotted. Green solid line; normal conditions; green dashed line, in the absence of EGFR internalisation; red dotted line, in the absence of EGFR internalisation and Ras activation; blue dotted line, in the absence of EGFR internalisation and Rap1 activation. The roles of Ras and Rap1 in EGF- and NGF-dependent ERK activation in silico (h-j). Concentration of the activated Ras or Rap1 was fixed at the basal level, and then simulations were run with (h) EGF (10 ng/ml) and (i) NGF (10 ng/ml), and phosphorylation of ERK was plotted. Blue line, normal conditions; green line, without Rap1 activation; red line, without Ras activation. (j) Rap1 activation depends on the affinity of FRS2 for the phosphorylated receptors. The dissociation constant of FRS2 for phosphorylated TrkA was set at 20, 50, 100, 200, 500 or 1000 nM. Then, the constant NGF stimulus (10 ng/ml) was given and the activation of Rap1 was plotted. The black, blue, cyan, green, orange and red lines indicate the Rap1 activation with 20, 50, 100, 200, 500 or 1000 nM of the dissociation constant of FRS2 for phosphorylated TrkA, respectively. Green dashed line indicates the Rap1 activation in response to EGF (10ng/ml) in silico where the affinity of FRS2 for phosphorylated EGFR was 200 nM (Fig. 2d). Note that 20 and 200 nM were the original dissociation constants of FRS2 for phosphorylated TrkA and EGFR in silico, respectively (Table S1).

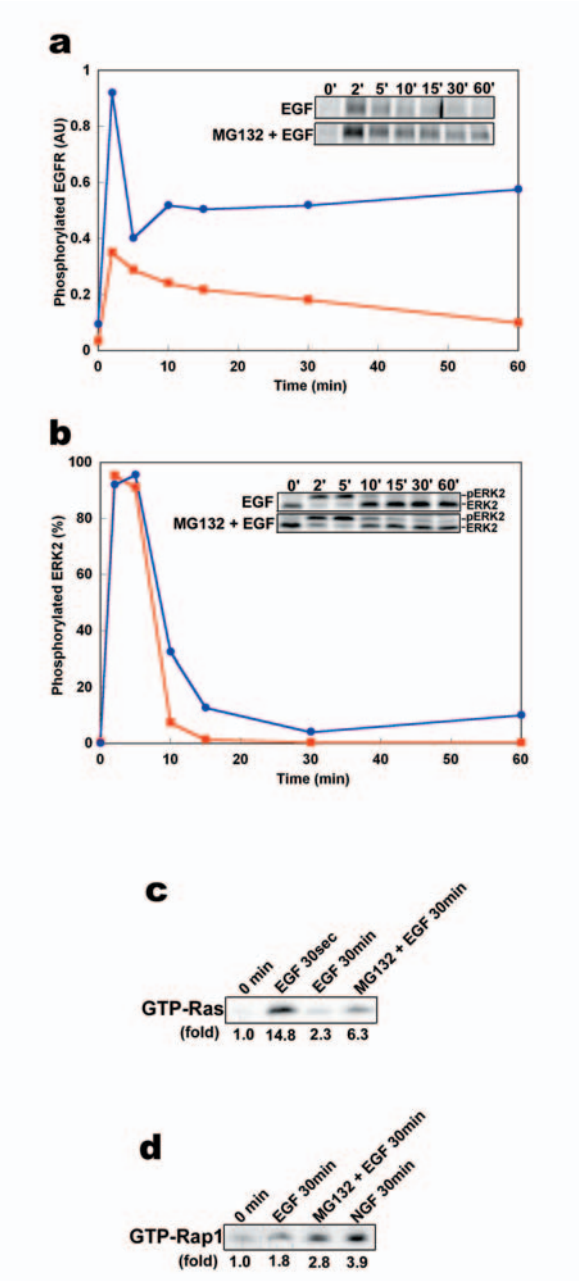

Figure S4 Sustained Ras, Rap1 and ERK activation in response to the sustained phosphorylated EGFR. (a, b) Fifty μM of MG-132, a proteasome inhibitor, was added for 1h, then PC12 cells were stimulated with EGF (10ng/ml). After stimulation, phosphorylated EGFR (a) and phosphorylated ERK2 (b) were measured. Blue and red lines indicate the responses in the presence or absence of MG-132, respectively. MG-132 alone did not affect the amounts of total and phosphorylated EGFR during incubation for 120 min (data not shown). Sustained Ras (c) and Rap1 (d) activation in the presence of MG-132 at 30 min after stimulation under the same conditions in (a).

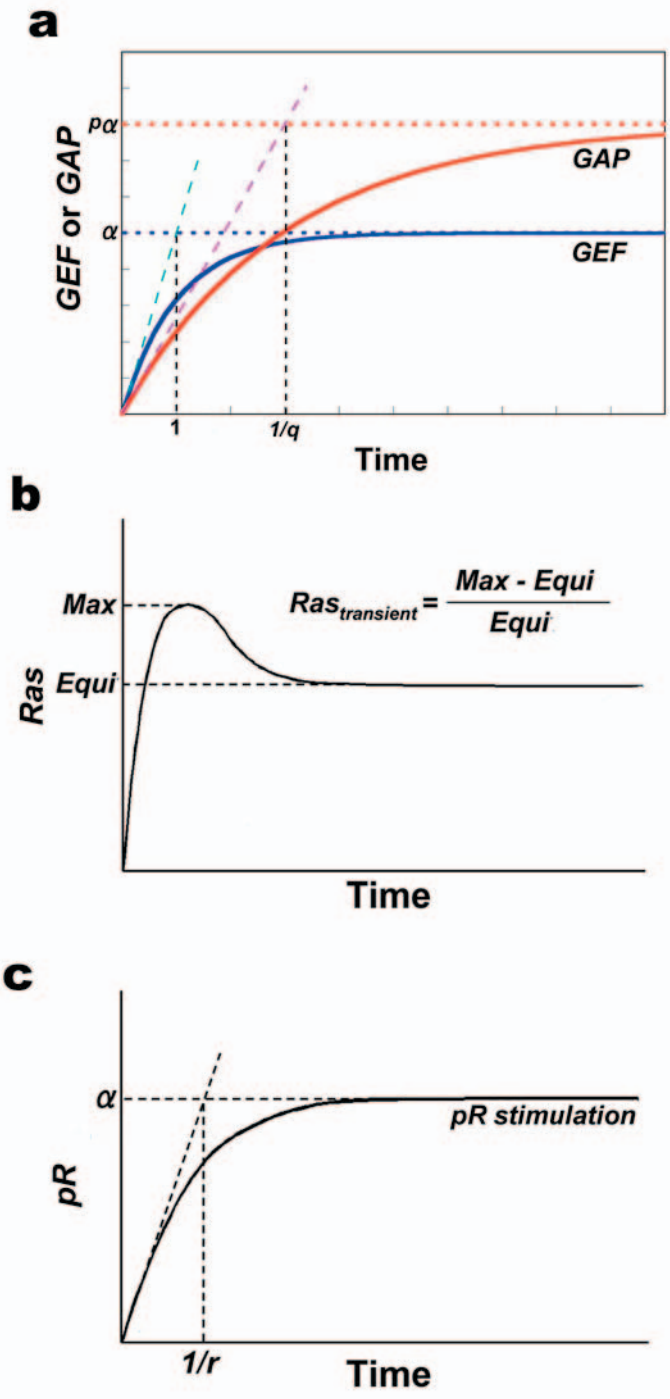

Figure S5 Transient Ras activation in the simple Ras model. (a) Schematic representation of the GEF activation and GAP activation in response to the constant pR stimulation. Here, 1/q can be regarded as the relative time constant of GAP activation compared to GEF activation. The dimensionless concentrations of GEF and GAP at steady state are given by α and $p\alpha$, respectively. Red and blue lines indicate GAP and GEF, respectively. (b) The definition of the characteristics of the transient Ras activation. The relative amplitude of the transient Ras activation compared to that at steady state was defined by Rastransinet, which is given by Rastransinet=(Max-Equi)/Equi (Appendix). Here, the transient Ras activation was defined by Rastransinet >0. (c) Increasing pR stimulation used in Fig. 6b and c. The pR stimulation was given by pR= α{1-exp(-rk2t)} (Appendix). Note that r corresponds to the increasing rate of pR. Time in a-c denotes t/k2.

Table S1a

Molecule-molecule interaction	Reaction number	kf (/s/μM)	kb (/s)	Notes
	1	1.0e-4 *	1.0e-4	Constrained by *in vivo* dynamics of EGFR (Fig. 2a)
	2	2.2833	0.0029666	[1,2]
	3	10	0.02	[3,4]
	4	4	0.001	[3,5,6]
	5	0.5	0.2	On the basis of[7], further constrained by *in vivo* dynamics of EGFR (Fig. 2a)
	6	0.05 *		On the basis of[7], further constrained by *in vivo* dynamics of EGFR (Fig. 2a)
	7	0.001 *		Constrained by *in vivo* dynamics of EGFR (Fig. 2a)
	8	10	0.2	[3,4]
	9	1 *		On the basis of[8], further constrained by *in vivo* dynamics of Ras (Fig. 2c)
	10	1	0.2	On the basis of[9], further constrained by EGF-dependent Rap1 activation (Fig. 2d)
	11	1 *		On the basis of[9], further constrained by EGF-dependent Rap1 activation (Fig. 2d)
	* denotes /s.			

Enzymatic reaction	Reaction number	Km (μM)	Vmax (/s)	Notes
	1	0.1	0.2	[10]

Initial concentration	Molecule	CoInit (μM)		Notes
	EGFR	0.3		[3]
	pro_EGFR	0.3	constant	[3,11]
	Shc	1		[3]
	c-Cbl	0.5		On the basis of[12], futher constrained by *in vivo* dynamics of EGFR (Fig. 2a)
	FRS2	1		[13]
	Dok	0.3		Constrained by *in vivo* dynamics of Ras (Fig. 2c)

1 French, A. R., Tadaki, D. K., Niyogi, S. K. & Lauffenburger, D. A. Intracellular trafficking of epidermal growth factor family ligands is directly influenced by the pH sensitivity of the receptor/ligand interaction. *J. Biol. Chem.* **270**, 4334-4340 (1995).

2 DeWitt, A. et al. Affinity regulates spatial range of EGF receptor autocrine ligand binding. *Dev. Biol.* **250**, 305-316 (2002).

3 Bhalla, U. S. & Iyengar, R. Emergent properties of networks of biological signaling pathways. *Science* **283**, 381-387 (1999).

4 Sasaoka, T., Langlois, W. J., Leitner, J. W., Draznin, B. & Olefsky, J. M. The signaling pathway coupling epidermal growth factor receptors to activation of p21ras. *J. Biol. Chem.* **269**, 32621-32625 (1994).

5 Kholodenko, B. N., Demin, O. V., Moehren, G. & Hoek, J. B. Quantification of short term signaling by the epidermal growth factor receptor. *J. Biol. Chem.* **274**, 30169-30181 (1999).

6 Schoeberl, B., Eichler-Jonsson, C., Gilles, E. D. & Muller, G. Computational modeling of the dynamics of the MAP kinase cascade activated by surface and internalized EGF receptors. *Nat. Biotechnol.* **20**, 370-375 (2002).

7 Levkowitz, G. et al. Ubiquitin ligase activity and tyrosine phosphorylation underlie suppression of growth factor signaling by c-Cbl/Sli-1. *Mol. Cell* **4**, 1029-1040 (1999).

8 Rozakis-Adcock, M. et al. Association of the Shc and Grb2/Sem5 SH2-containing proteins is implicated in activation of the Ras pathway by tyrosine kinases. *Nature* **360**, 689-692 (1992).

9 Wu, Y., Chen, Z. & Ullrich, A. EGFR and FGFR signaling through FRS2 is subject to negative feedback control by ERK1/2. *Biol. Chem.* **384**, 1215-1226 (2003).

10 Jones, N. & Dumont, D. J. Recruitment of Dok-R to the EGF receptor through its PTB domain is required for attenuation of Erk MAP kinase activation. *Curr. Biol.* **9**, 1057-1060 (1999).

11 Starbuck, C. & Lauffenburger, D. A. Mathematical model for the effects of epidermal growth factor receptor trafficking dynamics on fibroblast proliferation responses. *Biotechnol. Prog.* **8**, 132-143 (1992).

12 Kao, S., Jaiswal, R. K., Kolch, W. & Landreth, G. E. Identification of the mechanisms regulating the differential activation of the mapk cascade by epidermal growth factor and nerve growth factor in PC12 cells. *J. Biol. Chem.* **276**, 18169-18177 (2001).

13 Yamada, S., Taketomi, T. & Yoshimura, A. Model analysis of difference between EGF pathway and FGF pathway. *Biochem. Biophys. Res. Commun.* **314**, 1113-1120 (2004).

Table S1b

Molecule-molecule interaction	Reaction number	kf (/s/μM)	kb (/s)	Notes
	1	8.333e-4 *	2.7778e-4	[1]
	2	6.2	6.4e-5	On the basis of[2], further constrained by *in vivo* dynamics of TrkA (Fig. 2b)
	3	1 *		Constrained by *in vivo* dynamics of TrkA (Fig. 2b)
	4	6.3e-4 *		On the basis of[1], further constrained by *in vivo* dynamics of TrkA (Fig. 2b)
	5	4.2e-4 *		On the basis of[1], further constrained by *in vivo* dynamics of TrkA (Fig. 2b)
	6	10	0.2	On the basis of[3], further constrained by *in vivo* dynamics of Ras (Fig. 2c)
	7	5	0.1	On the basis of[3], further constrained by *in vivo* dynamics of Ras (Fig. 2c)
	8	0.1 *		On the basis of[4], further constrained by *in vivo* dynamics of Ras (Fig. 2c)
	9	2 *		On the basis of[5], further constrained by *in vivo* dynamics of Rap1 (Fig. 2d)
	10	0.0022 *		Constrained by *in vivo* dynamics of TrkA (Fig. 2b)
	* denotes /s.			

Enzymatic reaction	Reaction number	Km (μM)	Vmax (/s)	Notes
	1	0.1	0.02	On the basis of[6], further onstrained by *in vivo* dynamics of Ras (Fig. 2c)

Initial concentration	Molecule	CoInit (μM)		Notes
	TrkA	0.061894		[7]
	pro_TrkA	0.020631	constant	[1]

1 Jullien, J., Guili, V., Reichardt, L. F. & Rudkin, B. B. Molecular kinetics of nerve growth factor receptor trafficking and activation. *J. Biol. Chem.* **277**, 38700-38708 (2002).

2 Mahadeo, D., Kaplan, L., Chao, M. V. & Hempstead, B. L. High affinity nerve growth factor binding displays a faster rate of association than p140trk binding. Implications for multi-subunit polypeptide receptors. *J. Biol. Chem.* **269**, 6884-6891 (1994).

3 Farooq, A., Plotnikova, O., Zeng, L. & Zhou, M. M. Phosphotyrosine binding domains of Shc and insulin receptor substrate 1 recognize the NPXpY motif in a thermodynamically distinct manner. *J. Biol. Chem.* **274**, 6114-6121 (1999).

4 Gatti, A. Divergence in the upstream signaling of nerve growth factor (NGF) and epidermal growth factor (EGF). *Neuroreport* **14**, 1031-1035 (2003).

5 Kao, S., Jaiswal, R. K., Kolch, W. & Landreth, G. E. Identification of the mechanisms regulating the differential activation of the mapk cascade by epidermal growth factor and nerve growth factor in PC12 cells. *J. Biol. Chem.* **276**, 18169-18177 (2001).

6 Jones, N. & Dumont, D. J. Recruitment of Dok-R to the EGF receptor through its PTB domain is required for attenuation of Erk MAP kinase activation. *Curr. Biol.* **9**, 1057-1060 (1999).

7 Esposito, D. et al. The cytoplasmic and transmembrane domains of the p75 and Trk A receptors regulate high affinity binding to nerve growth factor. *J. Biol. Chem.* **276**, 32687-32695 (2001).

Table S1c

Molecule-molecule interaction	Reaction number	kf (/s/μM)	kb (/s)	Notes
	1	0.03	0.0168	[1]
	2	10	0.2	[1,2]
	3	0.005 *		[2]
	4	0.002 *		Constrained by *in vivo* dynamics of SOS (Fig. S2g, h)
	5	0.12	0.01	[3]
	6	0.002 *	1.0e-5	Constrained by *in vivo* dynamics of Ras (Fig. 2c)
	7	1.667e-4 *		[4]
	* denotes /s.			

Enzymatic reaction	Reaction number	Km (μM)	Vmax (/s)	Notes
	1	0.02	2	[5]
	2	25.641	1	[6]
	3	1	10	[7]

Initial concentration	Molecule	CoInit (μM)		Notes
	SOS	0.1		[6]
	Grb2	1		[6]
	RasGAP	0.1		[8]
	Ras	0.1		[6]

1 Chook, Y. M., Gish, G. D., Kay, C. M., Pai, E. F. & Pawson, T. The Grb2-mSos1 complex binds phosphopeptides with higher affinity than Grb2. *J. Biol. Chem.* **271**, 30472-30478 (1996).

2 Sasaoka, T., Langlois, W. J., Leitner, J. W., Draznin, B. & Olefsky, J. M. The signaling pathway coupling epidermal growth factor receptors to activation of p21ras. *J. Biol. Chem.* **269**, 32621-32625 (1994).

3 Kuriyan, J. & Cowburn, D. Modular peptide recognition domains in eukaryotic signaling. *Annu. Rev. Biophys. Biomol. Struct.* **26**, 259-288 (1997).

4 Kawata, M. et al. A novel small molecular weight GTP-binding protein with the same putative effector domain as the ras proteins in bovine brain membranes. Purification, determination of primary structure, and characterization. *J. Biol. Chem.* **263**, 18965-18971 (1988).

5 Margarit, S. M. et al. Structural evidence for feedback activation by Ras.GTP of the Ras-specific nucleotide exchange factor SOS. *Cell* **112**, 685-695 (2003).

6 Bhalla, U. S. & Iyengar, R. Emergent properties of networks of biological signaling pathways. *Science* **283**, 381-387 (1999).

7 Gideon, P. et al. Mutational and kinetic analyses of the GTPase-activating protein (GAP)-p21 interaction: the C-terminal domain of GAP is not sufficient for full activity. *Mol. Cell. Biol.* **12**, 2050-2056 (1992).

8 Schoeberl, B., Eichler-Jonsson, C., Gilles, E. D. & Muller, G. Computational modeling of the dynamics of the MAP kinase cascade activated by surface and internalized EGF receptors. *Nat. Biotechnol.* **20**, 370-375 (2002).

Table S1d

Molecule-molecule interaction	Reaction number	kf (/s/μM)	kb (/s)	Notes
	1	1	0.002	[1]
	2	1	0.2	[2]
	3	0.005 *		Constrained by *in vivo* dynamics of Rap1 activation (Fig. 2d)
	4	1.166e-4 *		[3]
	* denotes /s.			

Enzymatic reaction	Reaction number	Km (μM)	Vmax (/s)	Notes
	1	0.01	0.024	On the basis of[4], further constrained by *in vivo* dynamics of Rap1 activation (Fig. 2d)
	2	1	2	[5]

Initial concentration	Molecule	CoInit (μM)		Notes
	C3G	0.5		Constrained by *in vivo* dynamics of Rap1 activation (Fig. 2d)
	Crk	1		Constrained by *in vivo* dynamics of Rap1 activation (Fig. 2d)
	Rap1	0.2		On the basis of[6], further constrained by *in vivo* dynamics of Rap1 activation (Fig. 2d)
	Rap1GAP	0.012		On the basis of[6], further constrained by *in vivo* dynamics of Rap1 activation (Fig. 2d)

1 Knudsen, B. S., Feller, S. M. & Hanafusa, H. Four proline-rich sequences of the guanine-nucleotide exchange factor C3G bind with unique specificity to the first Src homology 3 domain of Crk. *J. Biol. Chem.* **269**, 32781-32787 (1994).

2 Kuriyan, J. & Cowburn, D. Modular peptide recognition domains in eukaryotic signaling. *Annu. Rev. Biophys. Biomol. Struct.* **26**, 259-288 (1997).

3 Kawata, M. et al. A novel small molecular weight GTP-binding protein with the same putative effector domain as the ras proteins in bovine brain membranes. Purification, determination of primary structure, and characterization. *J. Biol. Chem.* **263**, 18965-18971 (1988).

4 Gotoh, T. et al. Identification of Rap1 as a target for the Crk SH3 domain-binding guanine nucleotide-releasing factor C3G. *Mol. Cell. Biol.* **15**, 6746-6753 (1995).

5 Daumke, O., Weyand, M., Chakrabarti, P. P., Vetter, I. R. & Wittinghofer, A. The GTPase-activating protein Rap1GAP uses a catalytic asparagine. *Nature* **429**, 197-201 (2004).

6 Polakis, P. G., Rubinfeld, B., Evans, T. & McCormick, F. Purification of a plasma membrane-associated GTPase-activating protein specific for rap1/Krev-1 from HL60 cells. *Proc. Natl. Acad. Sci. U.S.A.* **88**, 239-243 (1991).

Table S1e

Molecule-molecule interaction	Reaction number	kf (/s/μM)	kb (/s)	Notes
	1	60	0.5	[1]
	2	60	0.5	[1,2]
	3	60	0.5	[3]
	4	0.15 *		[1]
	5	10	0.075	[4]
	6	16.304	0.6	[1]
	* denotes /s.			

Enzymatic reaction	Reaction number	Km (μM)	Vmax (/s)	Notes
	1	0.16	0.5	[1]
	2	0.16	0.2	[1]
	3	0.16	0.3	[1]
	4	15.657	3	[1]
	5	0.02	0.06	[5]

Initial concentration	Molecule	CoInit (μM)		Notes
	c-Raf	0.5		[1]
	B-Raf	0.2		[1]
	MEK	0.68		[1]
	ERK	0.26		[1]
	PP2A	0.24		[1]
	MKP3	0.018		[1,6]

1 Bhalla, U. S. & Iyengar, R. Emergent properties of networks of biological signaling pathways. *Science* **283**, 381-387 (1999).

2 Yamamori, B. et al. Purification of a Ras-dependent mitogen-activated protein kinase kinase kinase from bovine brain cytosol and its identification as a complex of B-Raf and 14-3-3 proteins. *J. Biol. Chem.* **270**, 11723-11726 (1995).

3 Ohtsuka, T., Shimizu, K., Yamamori, B., Kuroda, S. & Takai, Y. Activation of brain B-Raf protein kinase by Rap1B small GTP-binding protein. *J. Biol. Chem.* **271**, 1258-1261 (1996).

4 Khokhlatchev, A. V. et al. Phosphorylation of the MAP kinase ERK2 promotes its homodimerization and nuclear translocation. *Cell* **93**, 605-615 (1998).

5 Zhao, Y. & Zhang, Z. Y. The mechanism of dephosphorylation of extracellular signal-regulated kinase 2 by mitogen-activated protein kinase phosphatase 3. *J. Biol. Chem.* **276**, 32382-32391 (2001).

6 Schoeberl, B., Eichler-Jonsson, C., Gilles, E. D. & Muller, G. Computational modeling of the dynamics of the MAP kinase cascade activated by surface and internalized EGF receptors. *Nat. Biotechnol.* **20**, 370-375 (2002).